

---

## Which spatial interpolators I should use? A case study applying to marine species

Rufino Marta <sup>1,2,3,\*</sup>, Albouy Camille <sup>1</sup>, Brind'Amour Anik <sup>1</sup>

<sup>1</sup> IFREMER - Centre Atlantique, French Research Institute for Exploitation of the Sea, Département Ecologie et Modèles pour l'Halieutique (EMH), Rue de l'Île d'Yeu - BP 21105, 44311 Nantes cedex 3, France

<sup>2</sup> Portuguese Institute for the Sea and the Atmosphere (IPMA), Division of Modelling and Management of Fisheries Resources, Av. Dr. Alfredo Magalhães Ramalho, 6, 1495-165 Lisboa, Portugal

<sup>3</sup> Centre of Statistics and its Applications (CEAUL), Faculty of Sciences, University of Lisbon, Portugal

\* Corresponding author : Marta Rufino, email address : [marta.rufino@ipma.pt](mailto:marta.rufino@ipma.pt)

---

### Abstract :

Species are spread in space, whereas sampling is sparse. Thus, to describe and map along environmental gradients, it is necessary to interpolate the species abundance. Considering the plethora of valid methods, the researcher gets easily puzzled to choose the most appropriate interpolation approach with reference to the ecological question being asked.

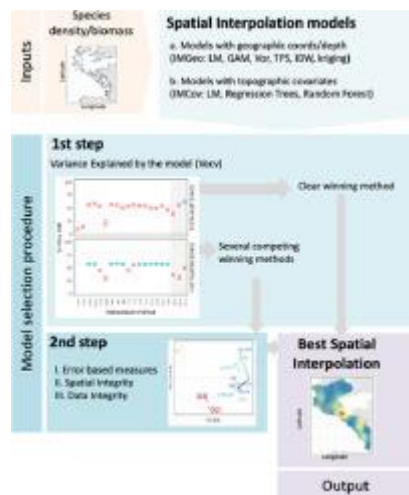
We propose a procedure to select among alternative spatial distribution models and we illustrate it with 175 marine species distributions (35 species \* 5 years). In a first step, the distribution of the variance explained by the predictive model (VEcv) given by 10-fold cross validation is estimated for each interpolation method. When the inter-quartile range of the VEcv distribution of the different methods overlap, the selection passes to a second step, using 11 measures belonging to three criteria: 1) error based measures, 2) spatial equivalence measures (center of gravity, inertia, isotropy and index of aggregation) and 3) measures based on the data integrity after interpolation, for example the percentage of area over the maximum sampled data.

We applied our approach to marine species sampled using either stratified random survey (trawl) or systematic survey (acoustic). We found that 87% of all species distributions had overlapping VEcv and thus passed the first selection. In the second selection step, the best method varied with species and year, although general additive model (GAM), Thin Plate Spline (TPS), Universal Kriging (UKr) and Random Forest (Rfor) performed better for the trawl data and TPS, Ordinary Kriging (OKri) and UKr for the acoustic data. Further, the results differed within methods (e.g. kriging neighborhood and type of kriging) and small modifications on the specifications can have a large impact on the surfaces produced.

The proposed approach 1) is accessible and intuitive, and does not require any complex software or sophisticated methodology; 2) shows exactly in what aspects each interpolation model is prevalent over the others and permits to make a decision accordingly to the objectives of the study; 3) takes into account

different criteria to evaluate each, properties of an interpolation method; 4) is universal and does not depend on the method used or the data characteristics. A detailed review on the subject is also included.

## Graphical abstract



## Highlights

► A new method was developed to select among spatial distribution models using 2-steps. ► The 1st step uses the variance explained by the predictive model (10-fold cross validation). ► The 2nd step uses 3 criteria: error based measures, spatial equivalence measures and data integrity. ► The method is illustrated using 175 marine species distributions (35 species x 5. years). ► The approach is accessible, clear, multi-criteria and is universal as it does not depend on the method used or the data characteristics.

**Keywords** : Spatial interpolation, Geostatistics, Machine learning, Spatial distribution, SDM, Review

56 Everything becomes clearer when it is presented in a figure. Maps of species distributions are  
57 required for numerous purposes, such as to visualize spatial variability, spot changes in the  
58 communities or provide estimations of variables of interest. Species distributions are mapped  
59 by interpolation, that is, predicting values at un-sampled areas using a modelling procedure  
60 applied to the sampled data. Ecological processes are inherent in species distributions (or spatial  
61 structure), such as those impacted by anthropogenic factors and climate change, and thus  
62 reflected in the respective maps. Coupled with species traits or phylogenetic information,  
63 species distribution maps can inform on the location of functional or phylogenetic hotspots.

64 Interpolated species distributions are widely used in a range of fields and applications, including  
65 regional biodiversity assessments, spatial conservation prioritization, evolutionary biology,  
66 epidemiology, global change biology and wildlife management (Araujo and Peterson, 2012).  
67 Given the importance of spatial interpolation, new and more powerful methods are developed  
68 on a regular basis and continuous/progressive evaluation of these statistical models is necessary  
69 (Austin, 2007).

70 There is a large body of literature on species distribution models (SDM, also known as  
71 bioclimatic envelope models, ecological niche models and habitat suitability models), that  
72 explore the relationship between geographical occurrences of species and corresponding  
73 environmental variables (Araújo and Guisan, 2006; Dormann et al., 2007; Elith and Leathwick,  
74 2009; Guisan and Zimmermann, 2000; Hui et al., 2013; Olden and Jackson, 2002). These are  
75 however, more challenging to apply on marine data to model than on its terrestrial counterparts.  
76 Marine fisheries data compared to its terrestrial counterpart (Lecours et al., 2016), typically have  
77 fewer sampling stations, in face of the large costs associated with the survey operations and  
78 cover irregular survey shape areas (e.g. 3-15 m depth along the coast). Further, marine species  
79 distributions are typically characterized by a large percentage of zero observations and a huge  
80 variability. Finally, the availability of environmental covariates in the marine field is generally  
81 scarcer, both in terms of geographic span and resolution, also due to difficulties associated with  
82 sampling. Thus, in face of this particularities of marine data, the challenges arisen by producing  
83 spatial models using this type of data have been often referred (Olden and Jackson, 2002).

84 So, the next question that naturally arises is which method to choose? It is widely recognized  
85 that there are no magical recipes to determine the perfect interpolation model. Undoubtedly,  
86 this should be focused on the data *per se*, laying on the statistical theoretical background and  
87 respective assumptions (Bivand et al., 2013; Cressie, 1993; Li and Heap, 2008; Sluiter, 2009;  
88 Wackernagel, 1998; Webster and Oliver, 2007). Several methods pass this first selection,  
89 however we need a framework accounting for model selection and evaluation to help decision  
90 making. Such decision is a complex issue, central to ecological modelling, with huge  
91 implications (Naimi and Araújo, 2016). Model selection involves evaluation, validation,  
92 performance, accuracy, skill, efficiency or robustness. Nevertheless these concepts are hard to  
93 disentangle and have been used with different meanings on the literature (reviewed in Bellocchi  
94 et al., 2010).

95 Generally, interpolators are compared using error based measurements, that is predicted *vs.*  
96 observed values, preferably obtained from cross-validation or jackknife processes (Li, 2016;  
97 reviewed by Li and Heap, 2008, 2011; Richter et al., 2012; Stow et al., 2009; Willmott et al.,  
98 2015). Using primarily error-based criteria, comparisons among spatial interpolators have been  
99 done in the field of meteorology (Aalto et al., 2013), air quality (Hoffman, 2015), soil (Gasch  
100 et al., 2015; Hengl et al., 2004, 2015), marine sediment (Diesing et al., 2014; Lark et al., 2016;  
101 Li et al., 2011), bathymetry (Amante and Eakins, 2016) and environmental sciences (Li and  
102 Heap, 2011, 2008). Among these, Mean Absolute Error (MAE, bias or a measure of average

103 error-magnitude) and Root Mean Squared Error (RMSE, for accuracy or over/under fitting) are  
104 the most commonly within the field of environmental sciences (Li and Heap, 2008; Richter et  
105 al., 2012; Willmott, 1982). However, as their magnitude depends on the scale/unit of the  
106 variable predicted, these are hardly comparable among variables or subjects. Further, most of  
107 these accuracy measures are algebraically related, being thus potentially redundant and  
108 collinear (Li, 2016; Li and Heap, 2011, 2008; Willmott et al., 2015). It has also been suggested  
109 the use of dimensionless measures, besides at least one error measure on the variable scale  
110 (modified coefficient of efficiency, Legates and McCabe Jr., 1999; coefficient of efficiency,  
111 Nash and Sutcliffe, 1970; index of agreement, Willmott, 1981, 1982; modified index of  
112 agreement, Willmott et al., 2012, 2015). Such approaches have been applied within the field  
113 of hydrology/climatology until recently, where Li (2016, 2017) revising Willmot's D,  
114 advocated its use as an universal tool to assess the accuracy of predictive models within  
115 environmental sciences, naming it Variance Explained by predictive models, estimated by  
116 cross-validation (VEcv), that is: how well a model is predicted, relative to the average of the  
117 observations (also called coefficient of efficiency, Nash and Sutcliffe, 1970 or G-value or  
118 goodness-of- prediction measure).

119 However, all these criteria often lead to overlapping results, that is several models having  
120 similar VEcv values, being difficult to select only one. Furthermore, these are based essentially  
121 on error measurements and do not take into account other fundamental aspects, such as spatial  
122 integrity (that is if the interpolation respects the spatial distribution of the data) or the spatial  
123 data limits of the interpolation relative to the original data. Additionally, whatever the criteria  
124 considered, it has long been demanded the establishment of a consistent and rationale set of  
125 procedures that should be used to compare spatial interpolation models (Fox 1981) (Willmott,  
126 1982).

127 The objective of the current work, is therefore, to develop a simple and accessible protocol to  
128 compare the results given by different spatial interpolating methods, that integrates important  
129 aspects for mapping marine species distribution, namely not only error measures, but also  
130 spatial and data integrity after interpolation. The proposed protocol was applied to compare 20  
131 interpolation methods applied to 35 species distributions from two typical fisheries surveys  
132 (trawl and acoustic), carried out during 5 years. The interpolation methods considered comprise  
133 approaches only using geographic coordinates and methods using depth and other topographic  
134 variables derived from bathymetry.

## 135 **Materials and Methods**

### 136 **DATA**

137 We considered two data sets for the species distributions case studies, one obtained from  
138 scientific groundfish bottom trawl surveys (EVHOE) and another from a scientific pelagic  
139 acoustic surveys (PELGAS).

140 The bottom trawl survey is carried out annually during Autumn in the North Atlantic  
141 ("Evaluation Halieutique de l'Ouest Européen, EVHOE cruise, RV Thalassa, IFREMER,"  
142 n.d.). It ranges from the Bay of Biscay up to the Celtic sea, with a randomly stratified sampling  
143 strategy, comprising from 119 to 153 stations/year ("Evaluation Halieutique de l'Ouest  
144 Européen, EVHOE cruise, RV Thalassa, IFREMER," n.d.)(map and location of sampling  
145 stations can be found in see Supplement 1). The biomass of the 29 fish species occurring more  
146 than 10 times/year during the survey and excluding the main pelagic species was used (see  
147 Supplement 1 for the species list names and further details on the survey). For the purpose of

148 this study we used data between 2011 and 2015 with an average of 198 sampling stations  
149 (number of hauls per year can be found in Supplement 1).  
150 The pelagic survey (Doray, M., Duhamel E. , Huret M. , Petitgas P., 2002; Doray M., Badts V.,  
151 Masse J., Duhamel E., Huret M., Doremus G., 2014) is an acoustic spring survey that aims at  
152 monitoring the Bay of Biscay pelagic ecosystem to inform fisheries and ecosystem  
153 management. Initially, PELGAS objective was to estimate biomass anchovy (*Engraulis*  
154 *encrasicolus*) and nowadays, the survey goals were extended to estimate the stocks of all the  
155 small pelagic fish species in the Bay of Biscay. From this survey we extracted the biomasses of  
156 six small pelagic fish species (see Supplement 1 for the species list and map), sampled over  
157 1345 to 1997 locations obtained from 29 acoustic radials perpendicular to the coast between  
158 2011 and 2015.  
159 In the simplest cases, interpolation can be carried out using only the geographic coordinates as  
160 explanatory variables. However, in marine systems bathymetry influences species spatial  
161 distribution and this information is available at global scale, and thus can be added to improve  
162 interpolation models. Bathymetry data was extracted from GEBCO data base and validated  
163 with depth data obtained during the EVHOE surveys (IMGeo). Additionally, other covariates  
164 derived from bathymetry can be included to improve interpolation models. Those additional  
165 covariates were added without referring to any specific ecological hypotheses, but likely  
166 serving as proxy of other unmeasured environmental variables. We extrapolated eleven  
167 covariates (IMCov) such as derived from bathymetry/elevation such as (Lecours et al., 2016;  
168 Wilson et al., 2007): slope, aspect, northerness, easternness, rough, profile curvature (surf.curv),  
169 bathymetric position index (TPI), terrain ruggedness index (TRI), surface flow (flowdir), local  
170 Moran I (moran) and distance to the nearest coast (dist.coast)(details of each variable and  
171 respective maps can be found in Supplement 2). Thus, all models using covariates (IMCov)  
172 were produced including all variables, whereas the final model, was produced with an automatic  
173 selection of these variables for each distribution.

## 174 INTERPOLATION METHODS

175 Seven families of methods were applied to both case studies, aiming not be exhaustive: linear  
176 models (LM), general additive models (GAM), Inverse Distance Weighting (IDW), Thin Plate  
177 Spline (TPS), VORonoi triangulation (VOR), Kriging (Kr) and stochastic Conditional  
178 Simulation (CSim) for the methods using just geographic coordinates and eventually depth  
179 (dep)(IMGeo) and three families of methods using the 11 bottom topographical variables  
180 (IMCov): multiple regression (GLM), Regression Tree (RTre) and Random Forest (RFor)  
181 (Hengl et al., 2015, 2007, 2004, 2003; Li et al., 2011)(Supplement 3). Additionally, we used  
182 several alternatives on some methods, intended to quantify the within-model and between-  
183 model variability (Araújo and Guisan, 2006), namely considering only geographic variables as  
184 covariates or adding depth as well (GAMl/ GAMd, MKri/ UKri), changing kriging  
185 neighborhood (OK03/ OK05/ OK07/ OK10/ OK20/ OK30 or the fitting procedure as automatic  
186 vs. manual (OKri/MKri)). We provided a brief description of the methods used in Supplement  
187 3 whereas additional details can be found in the vast literature (Bivand et al., 2013; Cressie,  
188 1993; Fortin and Dale, 2005) and more precisely in two reviews on the subject (Li and Heap,  
189 2008; Sluiter, 2009).

## 190 CRITERIA FOR COMPARISON OF INTERPOLATORS

191 Three complementary criteria were used to compare and evaluate the accuracy of interpolation  
192 models: (i) error based measures, (ii) changes in the spatial structure due to interpolation and  
193 (iii) data integrity after interpolation.

### 194 1. Error based measures

195 Error indices were estimated using predicted and observed values obtained by ten-fold cross-  
196 validation (10-fold CV). Ten-fold cross-validation was done by randomly splitting the data into  
197 10 parts. We estimated the model using 9 of those 10 data set, whereas the observed values  
198 (10<sup>th</sup> split) are predicted using the model estimated. This process is repeated for each of the ten  
199 splits, obtaining predicted and observed values for the ten folds, which are then used to estimate  
200 the error measures. We performed a 10-fold CV, and instead of leave one out procedure, as this  
201 method has been considered to give too optimistic measures of error. The process of 10-fold  
202 CV was then repeated with a random split 100 times to obtain a distribution of the error indices.  
203 From predicted and observed values obtained by 10-fold, three measures were calculated: MAE  
204 (Mean Absolute Error), RMSE (Root Mean Squared Error) and the Variance explained by  
205 predicted models estimated using cross validation procedures (VEcv). For comparability with  
206 previous works, the MAE ( [0, ∞], the lower the better) and Root Mean Squared Error (RMSE,  
207 [0, ∞], the lower the better) were estimated (Richter et al., 2012).

$$208 \quad MAE = \frac{1}{n} \sum_{i=1}^n (|P_i - O_i|)$$
$$209 \quad RMSE = \sqrt{\frac{1}{n} \sum_{i=1}^n (P_i - O_i)^2}$$

210 VEcv a dimensionless measure, varies between 100 for an excellent model and -∞. VEcv lower  
211 than 0, indicates that the model is worse than the average and we rounded these values to -1 for  
212 visualization purposes.

$$213 \quad VEcv = 100 \times \left(1 - \frac{\sum (P_i - O_i)^2}{\sum (O_i - \bar{O})^2}\right)$$

214 To perform the first step of our selection procedure (Fig. 1), we estimated the average RMSE,  
215 MAE and VEcv from the distributions obtained by the 10-fold CV, along with the upper and  
216 lower quantiles of the VEcv (probability of 0.25 and 0.75). We classified the average VEcv  
217 following Li (2016), into: 1) very poor if VEcv ≤ 10%; 2), poor if 10 < VEcv ≤ 30%; 3), average  
218 30 < VEcv ≤ 50%; 4), good if 50 < VEcv ≤ 80%; 5) and excellent if VEcv > 80%.

219 To harmonize the interpolation with the other interpolators considered in this study (MAE,  
220 RMSE), we calculated an inversion of the VEcv (VEcv.inv = abs(VEcv/100-1)\*100), where  
221 the lowest value, indicates the worst the model.

### 222 2. Spatial integrity

223 Ideally, an interpolation method should preserve the geometrical properties of the data, and  
224 therefore its spatial structure. We evaluated changes in the data spatial structure due to  
225 interpolation using deviations on four spatial indicators, relative to its results on the sampled  
226 data. Four spatial indicators were considered in the current work, following the revision and

227 work of (Rufino et al., 2019). The center of gravity (CG) indicates the mean spatial location of  
 228 the population (Bez and Rivoirard, 2001; Woillez et al., 2009b). The Euclidean distance  
 229 between the CG estimated using the sampled data (without considering different areas of  
 230 influence for each sample) and the interpolated data was calculated. It was used as a measure  
 231 of the impact of interpolation on the geometric center of the distribution. The inertia represents  
 232 the spatial dispersion of the population around its CG, i.e. the mean square distance between  
 233 individual fish and the CG (Bez and Rivoirard, 2001; Woillez et al., 2009b). Isotropy/anisotropy  
 234 (isotropy) represents the dispersion shape of the inertia around the CG (i.e. round or ellipsoid),  
 235 and it is simply the ratio between the two inertia axes (Woillez et al., 2009a).  
 236 The Gini index quantifies the distribution's aggregation or concentration, and represents twice  
 237 the area between the identity function and the Lorenz curve. It is bounded between 1 and 0, and  
 238 the highest its value the most concentrated is the biomass in fewest samples.  
 239 To quantify geometric changes in the spatial distribution due to interpolation, the difference  
 240 between the spatial indicators calculated for the sampled data and the indicators calculated in  
 241 from the interpolated surfaces was estimated. Thus, the absolute difference between inertia (log  
 242 transformed for scaling), isotropy and Gini index of the interpolated surfaces and the respective  
 243 ones estimated on the sampled data ( $\Delta I = |I_{\text{sample}} - I_{\text{interpolation}}|$ ) were used as a measure of the  
 244 interpolation method spatial integrity. Therefore, the higher the value of the difference on these  
 245 spatial measures, the higher the shift relative to the sampled data's spatial structure cause by  
 246 the interpolation method, thus the worse its performance.

### 247 3. Data limits integrity

248 Ideally, an interpolation method should preserve the samples data integrity and not predict  
 249 values outside the data range or shifts in the mean biomass. To evaluate interpolator's data  
 250 integrity, we used four measures estimated on each interpolated surface:

- 251 1) a.pix\_under: relative area below/above minimum sampled biomass ( $\text{pix\_under} =$   
 252  $\text{abs}[(\#\text{pixels}[\max(B)_{\text{interpolation}} < \max(B)_{\text{sample}}] / \#\text{pixels}_{\text{interpolation}}] \times 100)$ );
- 253 2) a.pix\_over: relative area above/bellow maximum sampled prediction ( $\text{pix\_over}$ )  
 254 ( $\text{abspix\_over} = [(\#\text{pixels}[\max(B)_{\text{interpolation}} > \max(B)_{\text{sample}}] / \#\text{pixels}_{\text{interpolation}}] \times 100)$ );
- 255 3) a.mean\_perc: relative change on the predicted mean biomass ( $\text{mean\_perc} = \text{abs}[(\mu_{\text{interpolation}}$   
 256  $- \mu_{\text{sample}}) / \mu_{\text{sample}}] \times 100)$ );
- 257 4) a.over\_perc: relative change on the maximum prediction ( $\text{over\_perc} = \text{abs}[(\mu_{\text{interpolation}} -$   
 258  $\mu_{\text{sample}}) / \mu_{\text{sample}}] \times 100)$ );

259 Where  $B_{\text{interpolation}}$  is the interpolated biomass,  $B_{\text{sample}}$  is the samped biomass and  $\#\text{pixels}$ , the  
 260 number of pixels. As most of these measures were dimensionless, they can be compared among  
 261 studies and methods and interpret as follow: the higher the value, the wose the performance of  
 262 the interpolator (for comparability with the other indicators).

263 The eleven criteria were scaled such as the highest the value, the greatest the impact of the  
 264 interpolation on the spatial structure and data integrity or greater the errors, bias or accuracy.  
 265 Additionally, these criteria were not strongly correlated between each other, except for the  
 266 RMSE/MAE (which is expected algebraically), a.mean\_perc with a.over\_perc ( $r = -63\%$ ) and  
 267 CGdist with a.inertia ( $r = 58\%$ ). Further, these criteria were also not strongly correlated with  
 268 biomass, which is another desirable property. The correlation between indicators is shown in  
 269 supplement 4.

## 270    PROTOCOL TO COMPARE THE INTERPOLATORS

271    The 2-steps protocol proposed to compare spatial interpolators is summarized in Fig. 1.

272    First step:

273    a) Estimate the distribution of  $VE_{cv}$  obtained by 10-fold CV. Select the interpolation method  
274    with the highest average  $VE_{cv}$ ;

275    b) Calculate the interquartile range (IQR) of each  $VE_{cv}$  distribution (Q1, 25% and Q3, 75%);

276    c) Select all interpolation methods where the IQR overlaps with the interpolation method that  
277    showed highest  $VE_{cv}$ ;

278    d) If no other interpolation method IQR overlaps the highest  $VE_{cv}$  IQR, the decision is reached,  
279    and the best method is clear. Otherwise, we continue to the second step.

280    Second step:

281        a) Calculate all measures proposed above for each interpolation method: 3 error  
282        measures ( $VE_{cv}$ , MAE and RMSE), 4 spatial indicators (distance of the center of  
283        gravity, difference in inertia, isotropy and Gini index) and the 4 data integrity  
284        measures;

285        b) Do a principal component analysis (PCA), scaled and not centered on the indicators  
286        matrix for the distribution (species-year), that render the criteria ranges comparable,  
287        and that integrates all measures vs. all methods being evaluated;

288        c) The inverse of the distance between the methods loadings on the first two PCA axes  
289        relative to the center of the PCA, is then used to rank the interpolation methods; The  
290        PCA further shows concretely what aspects of the sampled data, the interpolation  
291        model is not respecting;

292    This protocol was applied to every species/year distribution, for all interpolation methods being  
293    assessed as a case study. All analyses were carried out using r-project. An R-script with a small  
294    simplified example is added in the supplement 5.

## 295    **Results**

### 296    FIRST SELECTION STEP: $VE_{CV}$ CRITERIA

297    Twenty two percent of the models performed very poorly, producing interpolated surfaces that  
298    were worse than the mean, as shown by the negative average of the variance explained by the  
299    predictive model ( $VE_{cv} < 0$  in 784 models; Fig. 2). The maximum variance explained by the  
300    predictive model of the interpolations ( $VE_{cv}$ ) was 86% (EVH0E.TRISESM.2013-Kr3 -



301 *Trisopterus esmarkii* in 2013). Three species/years showed negative VECv for all models, and  
302 thus were eliminated from further analysis (CONGCON.2011, 2012 - *Conger conger* and  
303 LOPHPIS.2014 - *Lophius piscatorius* from 2014).

304 The percentage of 'bad' models was higher for the bottom trawl survey data (EVHOE; 25%)  
305 than for the pelagic survey (PELGAS; 11% Fig. 2 and Fig. 3). For the bottom trawl survey,  
306 VECv was slightly higher for GAM, TPS, geostatistical models (Kri) and RFor. As for the  
307 pelagic surveys, IDW, TPS, geostatistical models (Kri) and RFor reach better results (Fig. 2  
308 and Fig. 3). However, overall good VECv were lower than 50%, except for the acoustic surveys.  
309 Only few species distributions sampled with the acoustic surveys attained 'excellent' VECv  
310 classes, whereas most distributions were classified as good for IDW, TPS, Kriging and RForest  
311 (Fig. 2). For the bottom trawl data, most models were classified as average or poor according  
312 to the VECv criteria (Fig. 2). LM1 and LM2 were systematically worse than the mean.

313 Overall, the use of bottom covariates did not improve the interpolation's VECv (Fig. 3). The  
314 variance explained by the predictive model (VEcv) varied more among species than between  
315 years (Fig. 4 and Fig. 5). However, for some benthic species the models using covariates  
316 showed higher VECv than models without covariates (e.g. CONGCON - *Conger conger*,  
317 PHYBLE- *Phycis blennoides*, SOLESOL - *Solea solea*, HELIDAC - *Helicolenus*  
318 *dactylopterus*, SCYOCAN - *Scyliorhinus canicula* and LEPIWHI - *Lepidorhombus*  
319 *whiffiagonis*) (Fig. 4). Overall best results were obtained by species sampled in the pelagic  
320 survey, *Trisopterus esmarkii* (TRISESM) and *Merlangius merlangus* (MERNMER) were  
321 exceptions to this, attaining also higher VECv in bottom trawl survey. Inter-annual variability  
322 of VECv varied across species, with species (e.g. *Sardina pilchardus* - SARDPIL or *Trisopterus*  
323 *minutus* - TRISMIN) showing very little change in the results among the years, whereas others  
324 such as *Trisopterus luscus* (TRISLUS), showing a more variable results, although overall the  
325 patterns observed in relation to each method, across the years were relatively stable, i.e. most  
326 of the years within species showed a similar results (Fig. 5). Kriging based methods showed  
327 very similar VECv between each other, independently of the neighborhood considered (between  
328 3 and 30 points, i.e. OK03-OK30), the fitting of the variogram manually (MKri) or  
329 automatically (OKri), using depth as covariate (UKri) or even with conditional simulation  
330 (CSim) (Fig. 5).

331 In 13% of the distributions the method with the highest VECv showed no-overlapping of the  
332 IQR with all remaining methods (23 cases representing 15 species, out of the 172 sp/year  
333 distributions)(Fig. 5). Within those, in 10 cases, RFor was the best method, 6 cases it was  
334 GAMd, 3 cases UKr, 2 cases IDW and 1 case TPS and MKr. *Sprattus sprattus* (SPRASPR) was  
335 the only species from the pelagic survey with one distribution showing a clear winning method  
336 on the first step. In none of the case studies all years for one species showed only one best  
337 method. Thus, in the remaining 149 case studies a second selection step was required.

## 338 SECOND SELECTION STEP: MULTIPLE CRITERIA

339 The best interpolation method according to each criteria varied widely across species-years,  
340 confirming that different aspects of the distributions are taken into account by each measure  
341 (Fig. 6; note that cases with ties were omitted). For example, RFor was the best method in terms  
342 of a.pix\_under, a.over.perc, CGdist, RMSE and MAE whereas UKri was the best according to  
343 a.mean\_perc and GAMd produced the maps with less deviations on the isotropy and with more  
344 similar aggregation (Gini index, Fig. 6). It is also clear the contrast between the results given  
345 by different kriging neighborhood in the best method by criteria (Fig. 6).

346 For a decision framework on the second step, all measures from each distribution were  
347 integrated using a principal component analysis, as illustrated for four species/years in Fig. 7.

348 The variance explained by PC1 was always above 90%, although PC2 also proportionated  
349 important information in discriminating the issues of the different interpolators relatively to the  
350 measures considered. In the given examples, for *Argentina* sp. From 2014 (ARGENT.2014),  
351 GAM and TPS methods showed highest deviations in terms of pixels under minimum whereas  
352 kriging and Rfor showed highest spatial distortion, although integrating all criteria the best  
353 method would be Kr30. Similar interpretation can be done for every species/year distribution,  
354 and thus conclude that *Callionymus lyra* in 2012 (CLAMLYR.2012) best method would be  
355 GAM, for *Conger conger* in 2015 (CONGCON.2015) would be Kr30 whereas for *Gadiculus*  
356 *argenteus* in 2013 (GADIARG.2013) would be Kr7.  
357 The results of the protocol on the interpolator selection procedure, given the two steps together  
358 are found in Fig. 8. As already mentioned, few case studies were resolved on the first step (grey  
359 boxes). The use of the multi-criteria privileged GAM, TPS, UKr and Rfor for the trawl data set  
360 and TPS, OKri and UKr for the acoustic data set. It is also evident that the results differed  
361 within methods (e.g. kriging neighborhood and type of kriging) showing that small  
362 modifications on the methods can have a large impact on the surfaces produced. Further, it is  
363 interesting to observe such a large disparity on the best method, not only between species but  
364 also across years for the same species.

## 365 Discussion

366 In the current work we develop a two-step procedure to aid researchers select the best  
367 interpolation method for their data. The method uses a multi-criteria approach, that considers  
368 error-based measures, changes in the spatial structure and data integrity after interpolation and  
369 permits to determine in which particular aspect the interpolation is failing. The two-step  
370 procedure was illustrated by comparing 20 interpolation methods applied to 175 distributions,  
371 i.e. 35 species obtained during five years (2011-2015) of a typical bottom trawl survey and a  
372 pelagic acoustic survey. In the first step of the selection procedure, all interpolation methods  
373 within the highest VEcv's interquartile ranges are selected. In 13% of the case-studies no other  
374 method had overlapping VEcv and thus, the selection is complete without having to go through  
375 a second step. However, in the remaining 87% of the cases multiple methods were within the  
376 best VEcv interquartile range and thus a second step was proposed, using additional criteria.  
377 The effect of the interpolation was then integrated using PCA from which an index was  
378 extracted to rank the quality of the interpolations.

379 In the current work we aimed to use the simplest and most available approach to summarise the indicators  
380 in the second step, and this is why the PCA was selected. However, other multivariate statistical methods  
381 besides PCA could be used as an alternative in future works. Furthermore, it is possible to use just the first  
382 component (instead of two as in the current work) or to use the suggested indicators *per se*. Further work is  
383 needed to develop this particular aspect.

384

385

## 386 OTHER SELECTION PROCEDURES

387 Hengl *et al.* (2013) considered that the selection of a mapping procedure should account for  
388 accuracy (considered to be measured by RMSE), bias (considered to be measured by MAE),  
389 robustness (model sensitivity — in how many situations would the algorithm completely fail /  
390 how much artifacts does it produces?), reliability (how good is the model in estimating the

391 prediction error, i.e. how accurate is the prediction variance considering the true mapping  
392 accuracy?) and computation burden (the time needed to complete predictions). Visual  
393 examination has been considered as equally important as accuracy measurements (Li et al.,  
394 2011), although it is largely subjective and not explicitly defined, consistent or repeatable (Stow  
395 et al., 2009). Model selection has involved evaluation, validation, performance, accuracy, skill,  
396 efficiency or robustness, although these concepts are hard to disentangle and have been used  
397 with different meanings on the literature (reviewed in Bellocchi et al., 2010). There is a clear  
398 absence of a unifying selection procedure for interpolation models, although the most recent  
399 works advocate the use of V<sub>Ecv</sub> as a universal tool (Li, 2016, 2017). However, in 87% of the  
400 distributions studied in the current work such approach was not sufficient to discriminate among  
401 the interpolation methods, in view of the strong overlap between the respective distributions.  
402 Further, the measures used for model selection should be explicit, with a straightforward  
403 meaning and if possible, integrate multiple desirable properties of the interpolation procedure.  
404 Similar to the current study, other authors have suggested that method selection should be multi-  
405 criteria (Stow et al., 2009) and that the use of a single error measure may lead to incorrect  
406 interpretation (Hoffman, 2015) .

#### 407 RMSE AND MAE

408 Each different measure comes with advantages and drawbacks. RMSE provides a measure of  
409 error size, but it is sensitive to outliers as it places a lot of weight on large errors (Hernandez-  
410 Stefanoni and Ponce-Hernandez, 2006). However, MAE and RMSE are among the best overall  
411 measures of model performance as they summarize the mean difference in the units of observed  
412 and predicted values (Willmott, 1982), although being highly correlated between each other,  
413 with biomass/occurrence and algebraically related. Variance explained by predictive model  
414 (V<sub>Ecv</sub>) has been recently considered as the best error based criteria to evaluate interpolators  
415 (Li, 2017, 2016). Our results indicate that this measure is straightforward to interpret and quick  
416 evaluate thus it was included in the procedure, but for comparison with previous works, RMSE  
417 and MAE were also incorporated. .

#### 418 CROSS VALIDATION

419 The error measures used to evaluate interpolation methods are traditionally estimated by cross  
420 validation procedures, either leave one out (LOO)(Kilibarda et al., 2014) or k-fold cross-  
421 validation (generally five or ten)(Davis, 1987; Li et al., 2011)(for a schematic overview of the  
422 re-sampling strategies for model validation see Richter et al., 2012). First of all we decided to  
423 not perform LOO cross-validation because in the case of skewness distributions and extreme  
424 values of the input data, this kind of cross-validation might produce strange outputs (Hengl,  
425 2009). Secondly in highly clustered spatial distribution (like the species distributions  
426 considered), k (number of subsets, typically 5 or 10) should be large enough so that the data  
427 into the k-subsets contains enough information on the whole model domain and the spatial  
428 structure (Augustin et al., 2013). In our study, after a preliminary test, it was concluded that 10-  
429 fold was a good compromise for marine species distribution (not reported for brevity).  
430 Additionally, as the results of cross-validation strongly depended on the way the data is split  
431 (folds), the process should be randomly repeated several times, and as consequence it is  
432 obtained a distribution of the measure, which can then be used to compare the model's V<sub>Ecv</sub>  
433 (like it was done in the first step of the procedure). It is important to note also that cross-  
434 validation is not necessarily independent, indeed, points used for cross-validation are subset of

435 the original sampling design. Consequently, if the original design is biased and/or non-  
436 representative, then also the cross-validation might not reveal the true accuracy of a technique  
437 (Hengl, 2009). Further, error-based measures estimated by cross-validation results can be  
438 corrupted for clustered data sets on interpolator comparison (Hengl et al., 2013), highlighting  
439 the importance of having additional criteria in the selection procedure when the decision is not  
440 evident.

441 Cross validation can also be used to define the spatial model (Fortin and Dale, 2005; Gaetan et  
442 al., 2010; Wackernagel, 1998) and kriging neighborhood (Paramo and Roa, 2003) within the  
443 geostatistical methods. This is particularly crucial, because the effectiveness of the kriging  
444 depends on how well the selected model fits the data (Fortin and Dale, 2005). There were only  
445 small changes in the variance explained by the predictive model observed between kriging  
446 computed with different neighborhood or to the process of defining the spatial model (manual  
447 vs. automatic), when compared to other methods, but large changes were observed when the  
448 other comparison criteria were included. For example, Gini index or the percentage of over  
449 predictions changed widely with kriging neighborhood. Such comparison can also provide an  
450 idea of the variation due to the parametrization between and within each different techniques,  
451 as recommended in Araújo & Guisan (Araújo and Guisan, 2006)(within-model vs. between-  
452 model comparisons). Thus, the proposed protocol can also be applied as a tool to improve model  
453 specification by within model comparison, in future works. Similarly, the effect of a more  
454 detailed parametrization of the other interpolation methods on the quality of the predictions  
455 cannot be ignored. The method developed can also be used for such parametrization, as it was  
456 explored in the current work for kriging.

## 457 SPATIAL AND DATA INTEGRITY

458 Spatial indicators have been develop with the aim of quantifying distribution's spatial patterns  
459 (Bez and Rivoirard, 2001; Woillez et al., 2009b, 2007), but have also been applied as a model  
460 validation tool, to compare the model's outputs with sampled data for example (e.g. Huret et  
461 al., 2010)(Rufino et al., 2018). Additionally, these metrics are particularly sensitive to  
462 interpolation (Rufino et al., 2019) and are well suited to assess the spatial integrity of the sample  
463 data, after interpolation. The four metrics selected in our study highlight shifts in the main  
464 spatial features of the distributions, namely its location (center of gravity), dispersion (inertia),  
465 direction (isotropy) and aggregation (Gini index). It is expected (similar to what is done for  
466 modelling procedures) that a better interpolator would cause a minimum effect on those spatial  
467 aspects, when compared with the sampled data, therefore preserving the data spatial integrity.  
468 Future works can assess the use of other spatial indicators, such as the index of collocation for  
469 example, that may potentially be interesting with this aim.

470 Similarly, a good interpolation method should preserve the data limits of the sampled data. This  
471 is often done within works of spatial analysis, but rarely mentioned and hardly quantified. All  
472 those measures used in the selection procedure were made relative to the area and in the same  
473 direction (i.e. the larger the value, the worst the mode) for comparability purposes.

474 These aspects together are of outmost importance for species distributions maps, and have  
475 never been systematized previously. It can be argued that some of these measures just report  
476 the intrinsic properties of the interpolation methods and thus could be inferred solely on  
477 theoretical grounds. For example, kriging methods tend to under-estimate the maximum  
478 biomass (Bivand et al., 2013; Cressie, 1993). The proposed measures evidence those properties,  
479 and make them accessible without requiring a strong expertise on spatial analyses. On the other  
480 way, some measures, for example those with reference to the spatial integrity, are much less  
481 evident to describe theoretically.

## 482 PURELY GEOGRAPHIC METHODS VS. METHODS USING COVARIATES

483 Purely geographic methods, i.e. using only geographic coordinates to produce spatial  
484 predictions (i.e. ordinary kriging, TPS, IDW, etc.) are essential for the cases where there is a  
485 belief that geographic processes are dominant over environmental ones or in the absence of  
486 adequate environmental predictors (Elith and Leathwick, 2009). In the majority of cases the  
487 purpose of the statistical modelling is the prediction of species distribution, whereas the  
488 relationships between species and the environment tend to be a secondary consideration  
489 (Austin, 2002; Guisan and Zimmermann, 2000). This is also the focus of the current work and  
490 probably the commonest situation in marine studies or fisheries management. Thus, the applied  
491 models with covariates used only topographic variables directly derivable from depth, which is  
492 widely available. Unlike on its terrestrial counterpart, the effect of bottom topography on fish  
493 distribution is seldom tackled in fisheries ecology (Giannoulaki et al., 2006, 2003). These  
494 features are further advantageous for being relatively stable through time on these areas  
495 (Maravelias, 1999)(unlike other environmental characteristics) thus being potentially  
496 interesting also for long term studies, where other variables are not available.  
497 It can be expected that topographic information of the sea bottom is more important for  
498 demersal species than for the pelagic ones. However, sea bottom topography features are known  
499 to be determinant for small pelagics species (Giannoulaki et al., 2006; Maravelias, 1999) and  
500 some of these species occur also near the sea bottom (e.g. *Scomber* sp. and *Trachurus*  
501 *trachurus*). However, the models done with topographic variables were not better than those  
502 using just geographic variables for any pelagic species, but it is imperative to see the marine  
503 environment as a continuous system where all aspects are connected, and thereby only  
504 manageable through an ecosystem approach (Cotter et al., 2009; Doray et al., 2018). Other  
505 relevant environmental variables such as temperature and productivity, would improve the  
506 models with covariates, but can be more species specific. When a set of ecological covariates  
507 is available, whatever these are, the current method is also applicable.  
508

## 509 SPATIAL AUTOCORRELATION

510 The notion of spatial autocorrelation is largely attributed to Tobler's 1st Law of Geography,  
511 "Everything is related to everything else, but near things are more related than distant things"  
512 (Tobler, 1970). Spatial autocorrelation is widely present in marine species species distribution  
513 and is an essential aspect to account for in spatial prediction (Dormann et al., 2007; Elith and  
514 Leathwick, 2009; Legendre, 1993). We verified using a large empirical data set that models  
515 accounting for spatial autocorrelation (i.e. geostatistical models) showed higher VECv overall  
516 both for the bottom trawl data and for the acoustic pelagic survey. This difference was more  
517 pronounced on the acoustic pelagic data, where the number of samples is also much higher and  
518 the spatial models of the variogram, better defined (pers. obs. MMR). Improving the spatial  
519 model definition increases the effectiveness of kriging (Fortin and Dale, 2005). This was also  
520 observed in Rufino *et al* (2006) using simulated data, where the precision and accuracy of the  
521 kriging predictions increased with the sample size, as well as the importance of spatial  
522 autocorrelation. On the other way, in some cases, high data variability may hamper the retrieval  
523 of the spatial models and mask spatial autocorrelation (Rufino et al., 2006).  
524 The clumped spatial patterns typical of marine species distribution can emerge simply as a result  
525 of the spatial autocorrelation of the environmental and of biotic processes (Legendre, 1993). In  
526 the current work, most species evidenced the presence of auto-correlation in the experimental

527 variogram model. Strong residual geographic patterning generally indicates that either key  
528 environmental predictors are missing, that the model is mis-specified or that geographic factors  
529 are influential (Elith and Leathwick, 2009). In a study as broad as the current one this would be  
530 a natural consequence as it was not the aim to explore the key environmental predictors of each  
531 species, nether to parametrise in detail each method. Recent works have shown excellent results  
532 on the application of combined methods (random forest + kriging) in other areas (Appelhans et  
533 al., 2015; Diesing et al., 2014; Hengl et al., 2015; Li et al., 2011, 2013, 2016), and thus it would  
534 be interesting to explore such applications to marine SDM on future works. Further, the  
535 selection protocol is extensible interpolation methods on the spatio-temporal domain.  
536 It is evident that the best interpolation changed widely across species and years, and thus in  
537 each case a detailed analysis is required. Furthermore, the fact that certain interpolation models  
538 performed better for some species in a certain dataset, does not imply that it will always perform  
539 better with other fisheries datasets (Davis, 1987). Nevertheless, our application of the selection  
540 protocol to the two surveys reveals general guidelines for the variability of the results given by  
541 different interpolation methods. It is clear that each model need to be parameterized in detail,  
542 individually and according to the species data for a proper spatial analysis and that neglecting  
543 ecological knowledge is a limiting factor in the use of statistical modelling to predict species  
544 distribution (Austin, 2002).  
545 We conclude that the proposed 2-step approach for method's selection has several benefits: 1)  
546 it is accessible and does not require any complex software or sophisticated method; 2) it is  
547 explicit in the sense that it evidences the benefits of each interpolation model relative to the  
548 others, empirically, that is on the maps produced and thus, permits to make a decision  
549 accordingly to the objectives of each study; 3) it takes into account different criteria, thus  
550 integrating several desirable properties of interpolation methods; 4) it does not depend on the  
551 method used or the data characteristics, thus being universal and can be applied to virtually any  
552 method developed in the future.  
553

## 554 **Acknowledgments**

555 The authors acknowledge all previous participants in EVHOE and PELGAS surveys, in  
556 particular Mathieu Doray and Pierre Petitgas for providing the data set used in this work and  
557 for several discussions on the subjects covered. Marta M. Rufino is funded by a *post-doctoral*  
558 *contract (researcher)* awarded by IFREMER and Agrocampus Ouest within the framework of  
559 the MSFD. The authors also acknowledge two anonymous referees for their useful comments  
560 on the manuscript.

561 **Data availability**

562 The data used in the current work can be located in

563 <https://campagnes.flotteoceanographique.fr/series/8/>

564 **References**

- 565 Aalto, J., Pirinen, P., Heikkinen, J., Venäläinen, A., 2013. Spatial interpolation of monthly  
566 climate data for Finland: comparing the performance of kriging and generalized additive  
567 models. *Theor. Appl. Climatol.* 112, 99–111. doi:10.1007/s00704-012-0716-9
- 568 Amante, C.J., Eakins, B.W., 2016. Accuracy of interpolated bathymetry in digital elevation  
569 models. *J. Coast. Res.* 76, 123–133. doi:10.2112/SI76-011
- 570 Appelhans, T., Mwangomo, E., Hardy, D.R., Hemp, A., Nauss, T., 2015. Evaluating machine  
571 learning approaches for the interpolation of monthly air temperature at. *Spat. Stat.* 14,  
572 91–113. doi:10.1016/j.spasta.2015.05.008
- 573 Araújo, M.B., Guisan, A., 2006. Five (or so) challenges for species distribution modelling. *J.*  
574 *Biogeogr.* 33, 1677–1688. doi:10.1111/j.1365-2699.2006.01584.x
- 575 Araujo, M.B., Peterson, A.T., 2012. Uses and misuses of bioclimatic envelope modeling.  
576 *Ecology* 93, 1527–1539. doi:10.1890/11-1930.1
- 577 Augustin, N.H., Trenkel, V.M., Wood, S.N., Lorange, P., 2013. Space-time modelling of blue  
578 ling for fisheries stock management. *Environmetrics* 24, 109–119. doi:10.1002/env.2196
- 579 Austin, M., 2007. Species distribution models and ecological theory: A critical assessment  
580 and some possible new approaches. *Ecol. Modell.* 200, 1–19.  
581 doi:10.1016/j.ecolmodel.2006.07.005
- 582 Austin, M.P., 2002. Spatial prediction of species distribution: an interface between ecological  
583 theory and statistical modelling. *Ecol. Modell.* 157, 101–118. doi:10.1016/S0304-  
584 3800(02)00205-3
- 585 Baddeley, A., Gregori, P., Mateu, J., Stoica, R., Stoyan, D., Bickel, E.P., Diggle, P., Fienberg,  
586 S., Gather, U., Baddeley, A., Stoyan, D., 2006. *Case Studies in Spatial Point Process*  
587 *Modeling*. Springer. doi:10.1007/0-387-31144-0
- 588 Bellocchi, G., Rivington, M., Donatelli, M., Matthews, K., 2010. Validation of biophysical  
589 models : issues and methodologies. *Agron. Sustain. Dev.* 30, 109–130.  
590 doi:10.1051/agro/2009001
- 591 Bez, N., Rivoirard, J., 2001. Transitive geostatistics to characterise spatial aggregations with  
592 diffuse limits: an application on mackerel ichthyoplankton. *Fish. Res.* 50, 41–58.  
593 doi:10.1016/S0165-7836(00)00241-1
- 594 Bivand, R., Pebesma, E., Gómez-Rubio, V., 2013. *Applied spatial data analysis with R*, Use  
595 *R*. Springer. doi:10.1007/978-0-387-78171-6
- 596 Cotter, J., Petitgas, P., Abella, A., Apostolaki, P., Mesnil, B., Politou, C.-Y., Rivoirard, J.,  
597 Rochet, M.-J., Spedicato, M.T., Trenkel, V.M., Woillez, M., 2009. Towards an  
598 ecosystem approach to fisheries management (EAFM) when trawl surveys provide the  
599 main source of information. *Aquat. Living Resour.* 22, 243–254.  
600 doi:10.1051/alr/2009025
- 601 Cressie, N.A.C., 1993. *Statistics for spatial data*, *Statistics for Spatial Data*. John Wiley &

602 Sons, New York. doi:10.1002/9781119115151

603 Dauvin, J.-C., Thiebaut, E., Gesteira, J.L.G., Ghertsos, K., Gentil, F., Ropert, M., Sylvand, B.,  
604 2004. Spatial structure of a subtidal macrobenthic community in the Bay of Veys  
605 (western Bay of Seine, English Channel). *J. Exp. Mar. Bio. Ecol.* 307, 217–235.  
606 doi:10.1016/j.jembe.2004.02.005

607 Davis, B.M., 1987. Uses and abuses of cross-validation in geostatistics. *Math. Geol.* 19, 241–  
608 248. doi:10.1007/BF00897749

609 Diesing, M., Green, S.L., Stephens, D., Lark, R.M., Stewart, H.A., Dove, D., 2014. Mapping  
610 seabed sediments: Comparison of manual, geostatistical, object-based image analysis  
611 and machine learning approaches. *Cont. Shelf Res.* 84, 107–119.  
612 doi:10.1016/j.csr.2014.05.004

613 Doray, M., Duhamel E. , Huret M. , Petitgas P., M.J., 2002. PELGAS. doi:10.18142/18

614 Doray M., Badts V., Masse J., Duhamel E., Huret M., Doremus G., P.P., 2014. Manuel des  
615 protocoles de campagne halieutique. Campagnes PELGAS (PELagiques GAScogne) /  
616 Manual of fisheries survey protocols. PELGAS surveys (PELagiques GAScogne).  
617 doi:10.13155/30259

618 Doray, M., Petitgas, P., Romagnan, J.B., Huret, M., Duhamel, E., Dupuy, C., Spitz, J.,  
619 Authier, M., Sanchez, F., Berger, L., Dorémus, G., Bourriau, P., Grellier, P., Massé, J.,  
620 2018. The PELGAS survey: Ship-based integrated monitoring of the Bay of Biscay  
621 pelagic ecosystem. *Prog. Oceanogr.* 166, 15–29. doi:10.1016/j.pocean.2017.09.015

622 Dormann, C.F., McPherson, J.M., Araújo, M.B., Bivand, R., Bolliger, J., Carl, G., Davies,  
623 R.G., Hirzel, A., Jetz, W., Kissling, W.D., Kuhn, I., Ohlemuller, R., Peres-Neto, P.R.,  
624 Reineking, B., Schroder, B., Schurr, F.M., Wilson, R., 2007. Methods to account for  
625 spatial autocorrelation in the analysis of species distributional data: a review. *Ecography*  
626 (Cop.). doi: 10.1111. doi:10.1111/j.2007.0906-7590.05171.x

627 Elith, J., Leathwick, J.R., 2009. Species distribution models: ecological explanation and  
628 prediction across space and time. *Annu. Rev. Ecol. Evol. Syst.* 40, 677–697.  
629 doi:10.1146/annurev.ecolsys.110308.120159

630 Evaluation Halieutique de l’Ouest Européen, EVHOE cruise, RV Thalassa, IFREMER, n.d.  
631 doi:10.18142/8

632 Evans JS, 2017. spatialEco. R package version 0.0.1-7.

633 Fortin, M.M.-J., Dale, M.R.T., 2005. Spatial analysis: a guide for ecologists, 4th ed.  
634 Cambridge University Press, Cambridge. doi:10.2277/0521804345

635 Gaetan, C., Guyon, X., Bleakley, K., 2010. Spatial Statistics and Modeling, Media. Springer.  
636 doi:10.1007/978-0-387-92257-7

637 Gasch, C.K., Hengl, T., Gräler, B., Meyer, H., Magney, T.S., Brown, D.J., 2015. Spatio-  
638 temporal interpolation of soil water, temperature, and electrical conductivity in 3D + T:  
639 The Cook Agronomy Farm data set. *Spat. Stat.* 14, 70–90.  
640 doi:10.1016/j.spasta.2015.04.001

641 Giannoulaki, M., Machias, A., Koutsikopoulos, C., Haralabous, J., Somarakis, S., Tsimenides,  
642 N., 2003. Effect of coastal topography on the spatial structure of the populations of small  
643 pelagic fish. *Mar. Ecol. Prog. Ser.* 265, 243–253. doi:10.3354/meps265243

644 Giannoulaki, M., Machias, A., Koutsikopoulos, C., Somarakis, S., 2006. The effect of coastal  
645 topography on the spatial structure of anchovy and sardine. *ICES J. Mar. Sci.* 63, 650–  
646 662. doi:10.1016/j.icesjms.2005.10.017

647 Guisan, A., Edwards Thomas C., J., Hastie, T., 2002. Generalized linear and generalized  
648 additive models in studies of species distributions: setting the scene. *Ecol. Modell.* 157,  
649 89–100. doi:10.1016/S0304-3800(02)00204-1

650 Guisan, A., Zimmermann, N.E., 2000. Predictive habitat distribution models in ecology. *Ecol.*  
651 *Modell.* 135, 147–186. doi:10.1016/S0304-3800(00)00354-9



652 Hengl, T., 2009. A Practical guide to Geostatistical Mapping, Scientific and Technical  
653 Research series. doi:10.1016/0277-9390(86)90082-8

654 Hengl, T., Geuvelink, G.B.M., Stein, A., 2003. Comparison of kriging with external drift and  
655 regression kriging. Technical note, ITC, Available on-line at  
656 [http://www.itc.nl/library/Academic\\_output/](http://www.itc.nl/library/Academic_output/). doi:10.1016/S0016-7061(00)00042-2

657 Hengl, T., Heuvelink, G., Stien, A., 2004. A generic frame work for the spatial prediction of  
658 soil variables based on regression-kriging. *Geoderma* 120, 75–93.  
659 doi:10.1016/j.geoderma.2003.08.018

660 Hengl, T., Heuvelink, G.B.M., Kempen, B., Leenaars, J.G.B., Walsh, M.G., Shepherd, K.D.,  
661 Sila, A., MacMillan, R.A., De Jesus, J.M., Tamene, L., Tondoh, J.E., 2015. Mapping soil  
662 properties of Africa at 250 m resolution: Random forests significantly improve current  
663 predictions. *PLoS One* 10, 1–26. doi:10.1371/journal.pone.0125814

664 Hengl, T., Heuvelink, G.B.M., Rossiter, D.G., 2007. About regression-kriging: From  
665 equations to case studies. *Comput. Geosci.* 33, 1301–1315.  
666 doi:10.1016/j.cageo.2007.05.001

667 Hengl, T., MacMillan, R.A., Nikolić, M., 2013. Mapping efficiency and information content.  
668 *Int. J. Appl. Earth Obs. Geoinf.* 22, 127–138. doi:10.1016/j.jag.2012.02.005

669 Hoffman, S., 2015. Assessment of prediction accuracy in autonomous air quality models.  
670 *Desalin. Water Treat.* 57, 1322–1326. doi:10.1080/19443994.2014.1002283

671 Hui, F.K.C., Warton, D.I., Foster, S.D., Dunstan, P.K., 2013. Species Distribution Models:  
672 Ecological Explanation and Prediction Across Space and Time vs. separate species  
673 distribution models. *Ecology* 94, 1913–1919. doi:10.1890/12-1322.1

674 Huret, M., Petitgas, P., Woillez, M., 2010. Dispersal kernels and their drivers captured with a  
675 hydrodynamic model and spatial indices: A case study on anchovy (*Engraulis*  
676 *encrasicolus*) early life stages in the Bay of Biscay. *Prog. Oceanogr.* 87, 6–17.  
677 doi:10.1016/j.pocean.2010.09.023

678 Kilibarda, M., Hengl, T., Heuvelink, G.B.M., Gräler, B., Pebesma, E., Perčec Tadič, M.,  
679 Bajat, B., 2014. Spatio-temporal interpolation of daily temperatures for global land areas  
680 at 1 km resolution. *J. Geophys. Res. Atmos.* 119, 2294–2313.  
681 doi:10.1002/2013JD020803

682 Lark, M., Dove, D., Green, S., Stewart, H., Marchant, B., Diesing, M., 2016. Uncertainty in  
683 predictions of seabed sediment classes based on grab samples and acoustic data.  
684 *Geophys. Res. Abstr.* 18.

685 Lecours, V., Dolan, M.F.J., Micallef, A., Lucieer, V.L., 2016. A review of marine  
686 geomorphometry, the quantitative study of the seafloor. *Hydrol. Earth Syst. Sci.* 20,  
687 3207–3244. doi:10.5194/hess-20-3207-2016

688 Legates, D.R., McCabe Jr., G.J., 1999. Evaluating the use of “goodness of fit” measures in  
689 hydrologic and hydroclimatic model validation. *Water Resour. Res.* 35, 233–241.  
690 doi:10.1029/1998WR900018

691 Legendre, P., 1993. Spatial autocorrelation: trouble or new paradigm? *Ecology* 74, 1659–  
692 1673. doi:10.2307/1939924

693 Legendre, P., Legendre, L., 1998. *Numerical ecology*, 2nd ed. Elsevier, Amsterdam.  
694 doi:10.1016/S0304-3800(00)00291-X

695 Li, J., 2017. Assessing the accuracy of predictive models for numerical data: Not  $r$  nor  $r^2$ ,  
696 why not? Then what? *PLoS One* 12, 1–16. doi:10.1371/journal.pone.0183250

697 Li, J., 2016. Assessing spatial predictive models in the environmental sciences: Accuracy  
698 measures, data variation and variance explained. *Environ. Model. Softw.* 80, 1–8.  
699 doi:10.1016/j.envsoft.2016.02.004

700 Li, J., Heap, A.D., 2011. A review of comparative studies of spatial interpolation methods in  
701 environmental sciences: Performance and impact factors. *Ecol. Inform.* 6, 228–241.

702 doi:10.1016/j.ecoinf.2010.12.003  
703 Li, J., Heap, A.D., 2008. A review of spatial interpolation methods for environmental  
704 scientists, Geoscience Australia.  
705 Li, J., Heap, A.D., Potter, A., Huang, Z., Daniell, J.J., 2011. Can we improve the spatial  
706 predictions of seabed sediments? A case study of spatial interpolation of mud content  
707 across the southwest Australian margin. *Cont. Shelf Res.* 31, 1365–1376.  
708 doi:10.1016/j.csr.2011.05.015  
709 Li, J., Justy, P., Siwabessy, W., Tran, M., Huang, Z., Heap, A.D., 2013. Predicting Seabed  
710 Hardness Using Random Forest in R, in: Elsevier (Ed.), *Data Mining Applications with*  
711 *R*. pp. 299–329. doi:10.1016/B978-0-12-411511-8.00011-6  
712 Li, J., Siwabessy, J., Tran, M., 2016. Selecting optimal random forest predictive models : a  
713 case study on predicting the spatial distribution of seabed hardness selecting optimal  
714 random forest predictive models: a case study on predicting the spatial distribution of  
715 seabed hardness. *PLoS One* 11, 1–29. doi:10.1371/journal.pone.0149089  
716 Maravelias, C.D., 1999. Habitat selection and clustering of a pelagic fish: effects of  
717 topography and bathymetry on species dynamics. *Can. J. Fish. Aquat. Sci.* 56, 437–450.  
718 doi:10.1139/f98-176  
719 Morfin, M., Bez, N., Fromentin, J.M., 2016. Habitats of ten demersal species in the Gulf of  
720 Lions and potential implications for spatial management. *Mar. Ecol. Prog. Ser.* 547, 219–  
721 232. doi:10.3354/meps11603  
722 Naimi, B., Araújo, M.B., 2016. Sdm: A reproducible and extensible R platform for species  
723 distribution modelling. *Ecography (Cop.)*. 39, 368–375. doi:10.1111/ecog.01881  
724 Nash, J.E., Sutcliffe, J. V, 1970. River flow forecasting through conceptual models part I-a  
725 discussion of principles. *J. Hydrol.* 10, 282–290. doi:10.1016/0022-1694(70)90255-6  
726 Nychka, D., 2016. *fields: Tools for Spatial Data*. doi:10.5065/D6W957CT  
727 Olden, J.D., Jackson, D.A., 2002. A comparison of statistical approaches for modelling fish  
728 species distributions. *Freshw. Biol.* 47, 1976–1995. doi:10.1046/j.1365-  
729 2427.2002.00945.x  
730 Paramo, J., Roa, R., 2003. Acoustic-geostatistical assessment and habitat-abundance relations  
731 of small pelagic fish from the Colombian Caribbean. *Fish. Res.* 60, 309–319.  
732 doi:10.1016/S0165-7836(02)00142-X  
733 Richter, K., Atzberger, C., Hank, T.B., Mauser, W., 2012. Derivation of biophysical variables  
734 from Earth observation data: validation and statistical measures. *J. Appl. Remote Sens.*  
735 6, 063557–1. doi:10.1117/1.JRS.6.063557  
736 Rufino, M.M., Bez, N., Brind’Amour, A., 2019. Influence of data pre-processing on the  
737 behavior of spatial indicators. *Ecol. Indic.* 99, 108–117.  
738 doi:10.1016/j.ecolind.2018.11.058  
739 Rufino, M.M., Bez, N., Brind’Amour, A., 2018. Integrating spatial indicators in the  
740 surveillance of exploited marine ecosystems. *PLoS One* 13, e0207538.  
741 doi:10.1371/journal.pone.0207538  
742 Rufino, M.M., Stelzenmüller, V., Maynou, F., Zauke, G.P., 2006. Assessing the performance  
743 of linear geostatistical tools applied to artificial fisheries data. *Fish. Res.* 82, 263–279.  
744 doi:10.1016/j.fishres.2006.06.013  
745 Sluiter, R., 2009. Interpolation methods for climate data literature review, KNMI intern  
746 rapport.  
747 Stow, C.A., Jolliff, J., McGillicuddy, D.J., Jr., c S.C.D., Allen, J.I., Friedrichs, M.A.M.,  
748 Rose, K.A., Wallhead, P., 2009. Skill assessment for coupled biological/physical models  
749 of marine systems. *J. Mar. Syst.* 76, 4–15. doi:10.1016/j.jmarsys.2008.03.011  
750 Thorson, J.T., Shelton, A.O., Ward, E.J., Skaug, H.J., 2015. Geostatistical delta-generalized  
751 linear mixed models improve precision for estimated abundance indices for West Coast

752 groundfishes. ICES J. Mar. Sci. 72, 1297–1310. doi:10.1093/icesjms/fsu243  
753 Tobler, W.R., 1970. A computer movie simulation urban growth in Detroit region. Econ.  
754 Geogr. 46, 234–240. doi:10.1126/science.11.277.620  
755 Wackernagel, H., 1998. Multivariate geostatistics: An introduction with applications., Second.  
756 ed. Springer-Verlag, Berlin. doi:10.1007/978-3-662-03550-4  
757 Webster, R., Oliver, M., 2007. Geostatistics for environmental scientists, 2nd ed. ed. John  
758 Wiley and Sons, New York. doi:10.1002/9780470517277  
759 Willmott, C.J., 1982. Some comments on the evaluation of model performance. Bull. Am.  
760 Meteorol. Soc. 1309–1313. doi:10.1175/1520-0477(1982)063<1309:SCOTEO>2.0.CO;2  
761 Willmott, C.J., 1981. On the validation of models. Phys. Geogr. 2, 184–194.  
762 doi:10.1080/02723646.1981.10642213  
763 Willmott, C.J., Robeson, S.M., Matsuura, K., 2012. A refined index of model performance.  
764 Int. J. Climatol. 32, 2088–2094. doi:10.1002/joc.2419  
765 Willmott, C.J., Robeson, S.M., Matsuura, K., Ficklin, D.L., 2015. Assessment of three  
766 dimensionless measures of model performance. Environ. Model. Softw. 73, 167–174.  
767 doi:10.1016/j.envsoft.2015.08.012  
768 Wilson, M.F.J., Connell, B.O., Guinan, J.C., Grehan, A.J., 2007. Multiscale terrain analysis of  
769 multibeam bathymetry data for habitat mapping on the continental slope.  
770 doi:10.1080/01490410701295962  
771 Woillez, M., Poulard, J.-C., Rivoirard, J., Petitgas, P., Bez, N., 2007. Indices for capturing  
772 spatial patterns and their evolution in time, with application to European hake  
773 (*Merluccius merluccius*) in the Bay of Biscay. ICES J. Mar. Sci. 64, 537–550.  
774 doi:10.1093/icesjms/fsm025  
775 Woillez, M., Rivoirard, J., Fernandes, P.G., 2009a. Evaluating the uncertainty of abundance  
776 estimates from acoustic surveys using geostatistical simulations. ICES J. Mar. Sci. 66,  
777 1377–1383. doi:10.1093/icesjms/fsp137  
778 Woillez, M., Rivoirard, J., Petitgas, P., 2009b. Notes on survey-based spatial indicators for  
779 monitoring fish populations. Aquat. Living Resour. 22, 155–164.  
780 doi:10.1051/alr/2009017  
781 Wood, N.S., 2006. Generalized Additive Models: An Introduction with R, Texts in Statistical  
782 Science Series. Chapman & Hall/CRC. doi:10.1201/9781315370279  
783 Zuur, A.F., Ieno, E.N., Smith, G.M., 2007. Analysing Ecological Data, Profiles of drug  
784 substances, excipients, and related methodology. Springer. doi:10.1016/B978-0-12-  
785 387667-6.00013-0  
786  
787

## FIGURE LEGENDS:

789 Fig. 1: Graphical abstract: Conceptual diagram of the method developed to compare the  
790 interpolators.

791 Fig. 2: Frequency of the variance explained by predictive model classes between spatial  
792 interpolation methods, for the bottom trawl survey (EVHOE, upper panel) and the acoustic  
793 pelagic survey (PELGAS, lower panel). Find further details on the methods codes in text.

794 Fig. 3 : Variance explained by the predictive model between spatial interpolation method's  
795 main families, by survey (blue triangles for pelagic survey, PELGAS and red bals for bottom  
796 trawl survey, EVHOE)(mean and respective 95% CI estimated using bootstrap). LM: linear  
797 model; GAM: generalised additive models; IDW: inverse distance weighting; Vor: voronoi  
798 triangulation; TPS: thin plate spline; Kri: kriging and conditional simulation; Covar: multiple  
799 regression, regreition tree and random forest (simple and mixed, i.e. with kriged residuals).  
800 Please find further details on the methods codes in the text.

801 Fig. 4 : Variance explained by the predictive model between species, for interpolation methods  
802 using topographic covariates (orange line with squares, IMCov) and for methods just using  
803 geographic coordinates and eventually depth (green line with diamonds, IMGeo). Filled  
804 symbols represent the species captured in the bottom trawl survey whereas open symbols  
805 indicate the acoustic pelagic survey. Mean and respective 95% CI estimated using bootstrap is  
806 represented. Species were ordered by IMGeo VEcv. Find further details on the species codes  
807 in the text.

808 Fig. 5: Variance explained by the model of each interpolation method (median), estimated by  
809 cross validation for all species-year distributions. Red points indicate that the interpolation  
810 method was within the best method interquartile range and red star indicate the best VEcv in  
811 each case whereas black dots indicate models that did not passed for thr second step. Grey  
812 shaded area correspond to methods carried out using the 11 topographic covariates (IMCov),  
813 whereas white background shows methods using only lat+long and some depth (IMGeo). Please  
814 find further details on the methods and species codes in the text.

815 Fig. 6: Distributions and methods that required the second step. Winning interpolation method  
816 according to each measure criteria (left panel; only cases where more than one method showing  
817 its VEcv within the highest method VEcv interquartile range were selected and situations with  
818 ties were excluded, i.e. several methods showing the same classification according to the  
819 criteria). Winning method for each measure-criteria by species-year distribution (right panel).  
820 Vertical grey line separates the methods using several covariates from the others. Please find  
821 further details on the criteria and methods codes in the text. The colour legend is represented in  
822 the barplot.

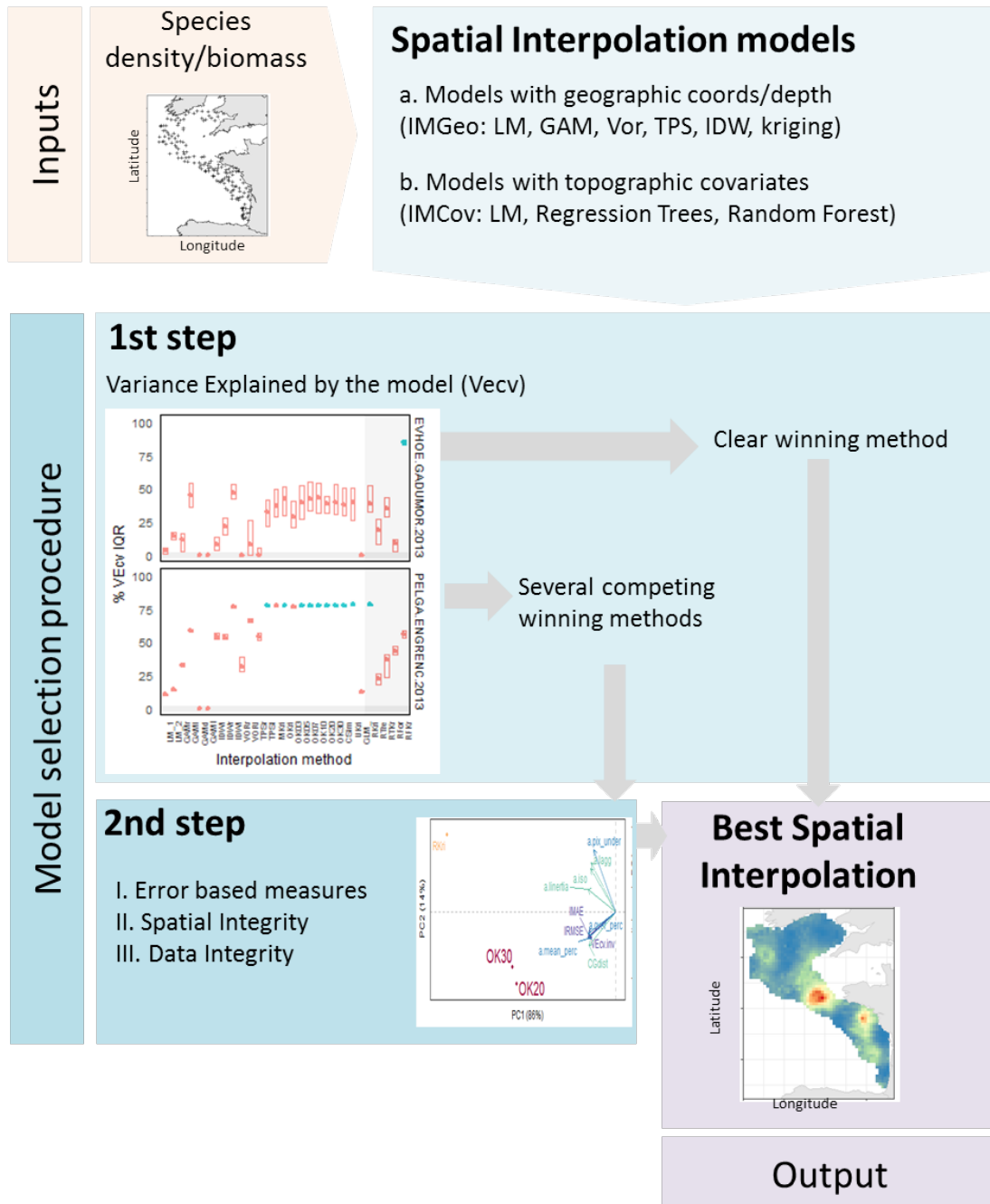
823 Fig. 7: Second step of the spatial interpolator's selection protocol applied to four case studies  
824 (2 bottom trawl, EVHOE and 2 acoustic pelagic, PELGAS). On the right side plots, the PCA  
825 shows where each interpolation method (represented with circles, orange-red coloured,  
826 according to the distance to the centre) failed according to the measures representing the three  
827 selection criteria (error-based in violet, spatial integrity in green and data integrity in blue). On  
828 the left panels, the inverse Euclidean distance to the centre of each method, provides the  
829 quantitative decision integrative measure. Please find the details of the code's labels in the text.

830 Fig. 8: Winning spatial interpolation method among the different approaches considered, for  
831 each case study (species-year distributions) according to the two step selection procedure (1<sup>st</sup>  
832 step using IQR VEcv identified with orange line and 2<sup>nd</sup> step, using the 3 criteria with 11  
833 measures, identified with blue line). Number of cases of each selected method by survey.  
834 Vertical grey line separates the methods using several covariates from the others. See further  
835 details of the species codes and methods on text. The colour legend is represented in the barplot.

836  
837

838 **Figures**

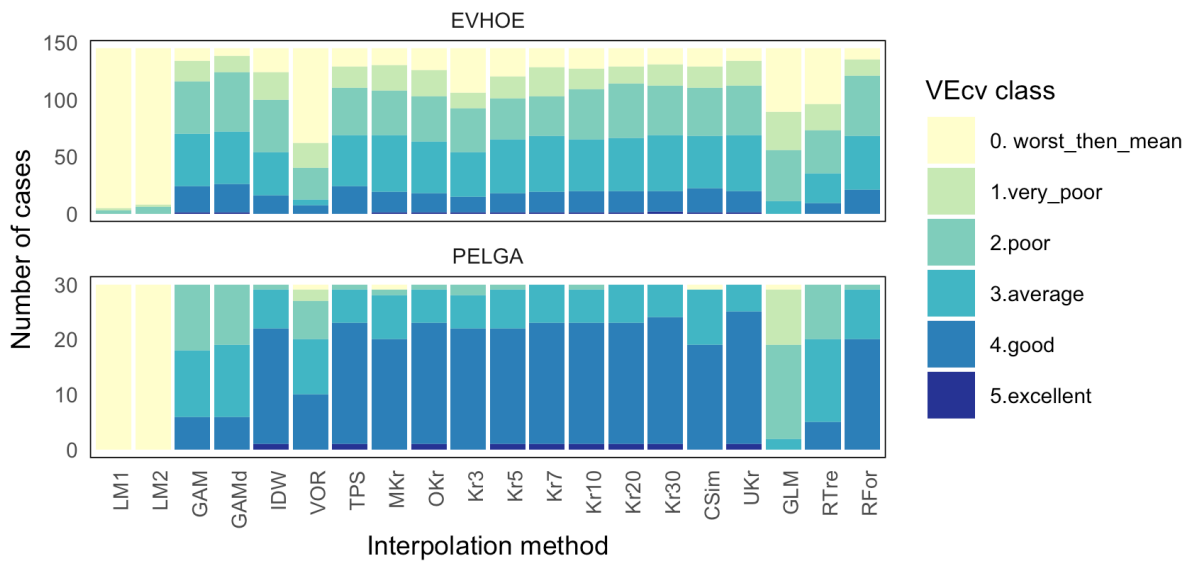
839 **Fig. 1**



840  
841

842

**Fig. 2: VEcv classes + RT**



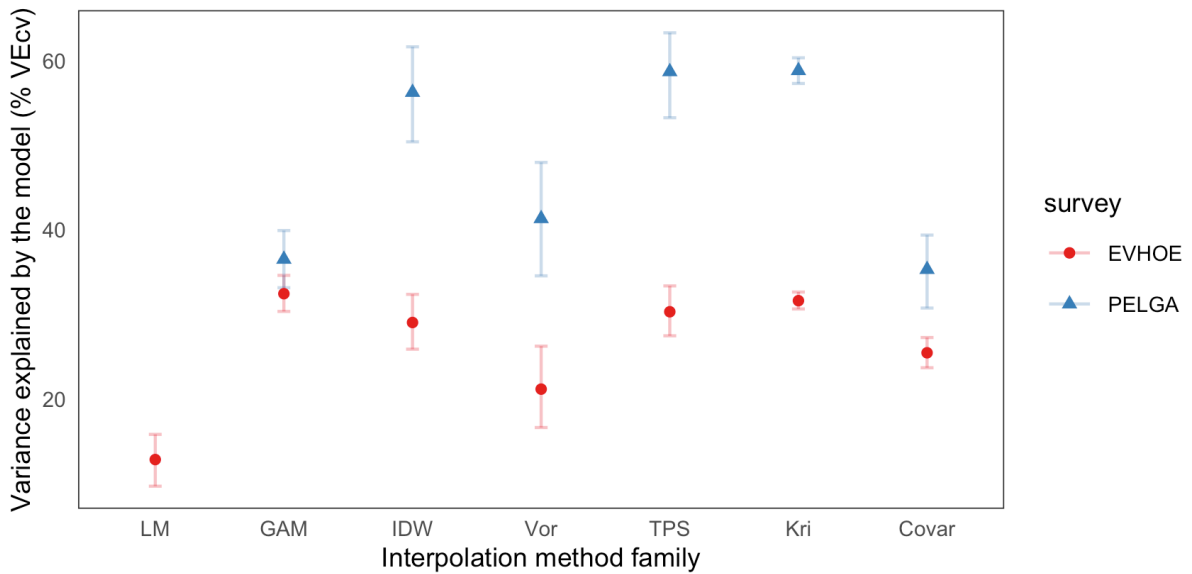
843

844

845

846

**Fig. 3: VEcv by family**



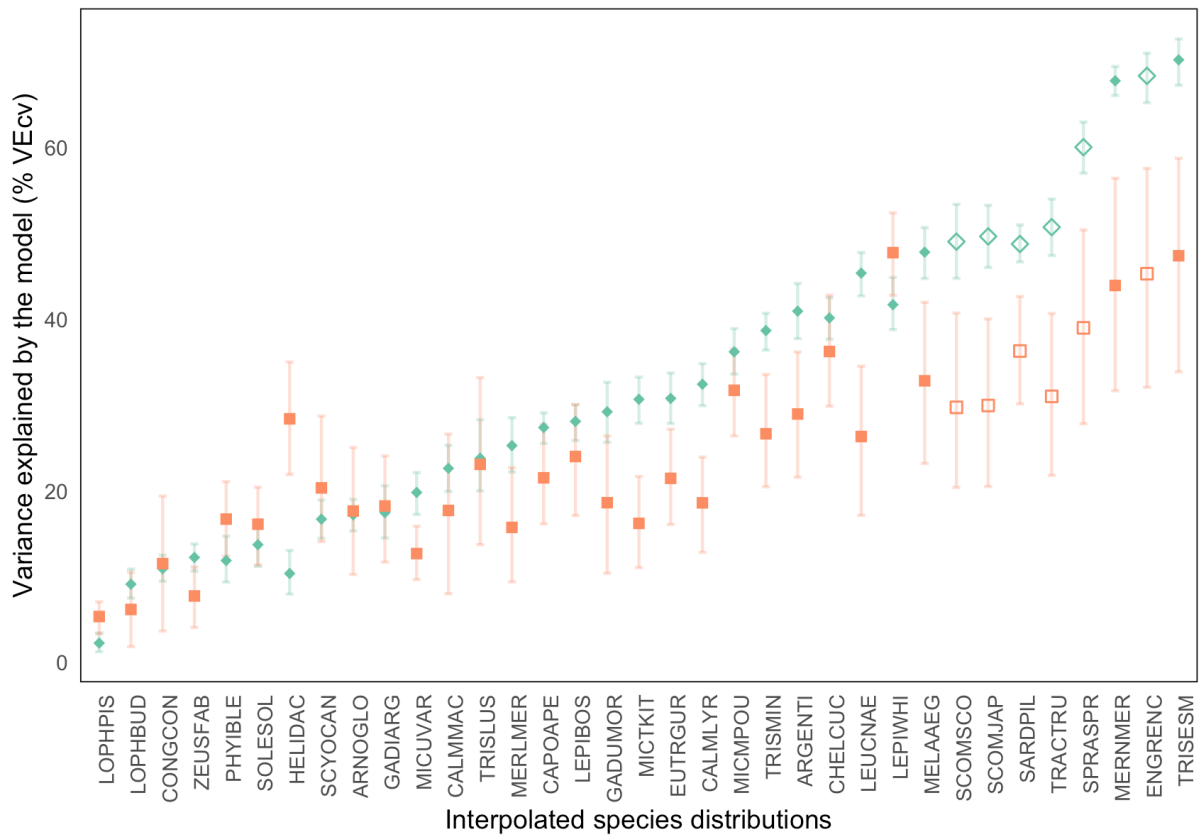
847

848

**Fig. 4: VEcv by Sp**

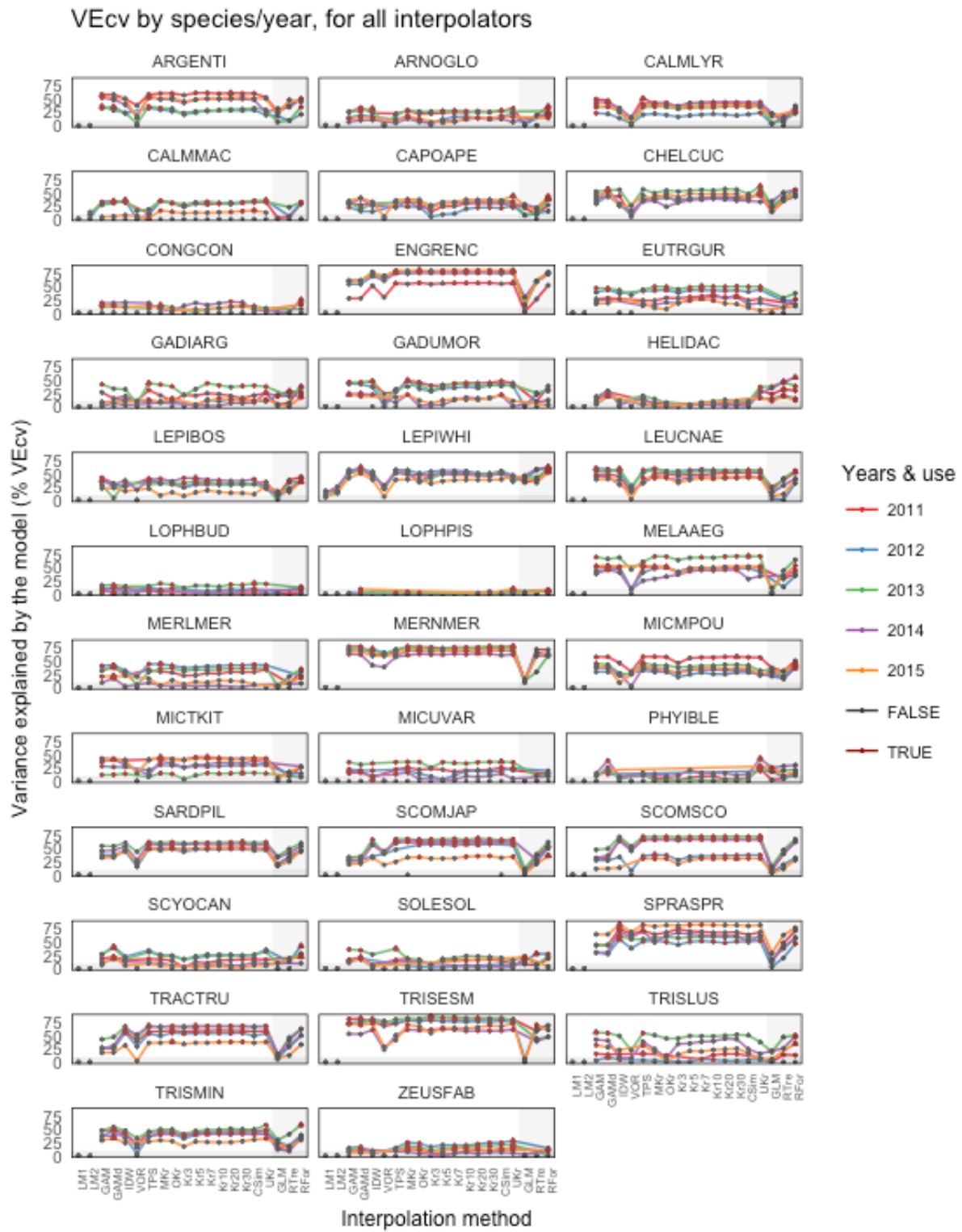
849

850



852  
853

**Fig. 5: all VECvs**



854  
855



Fig. 6: Best method according to each criteria (2<sup>nd</sup> step only).

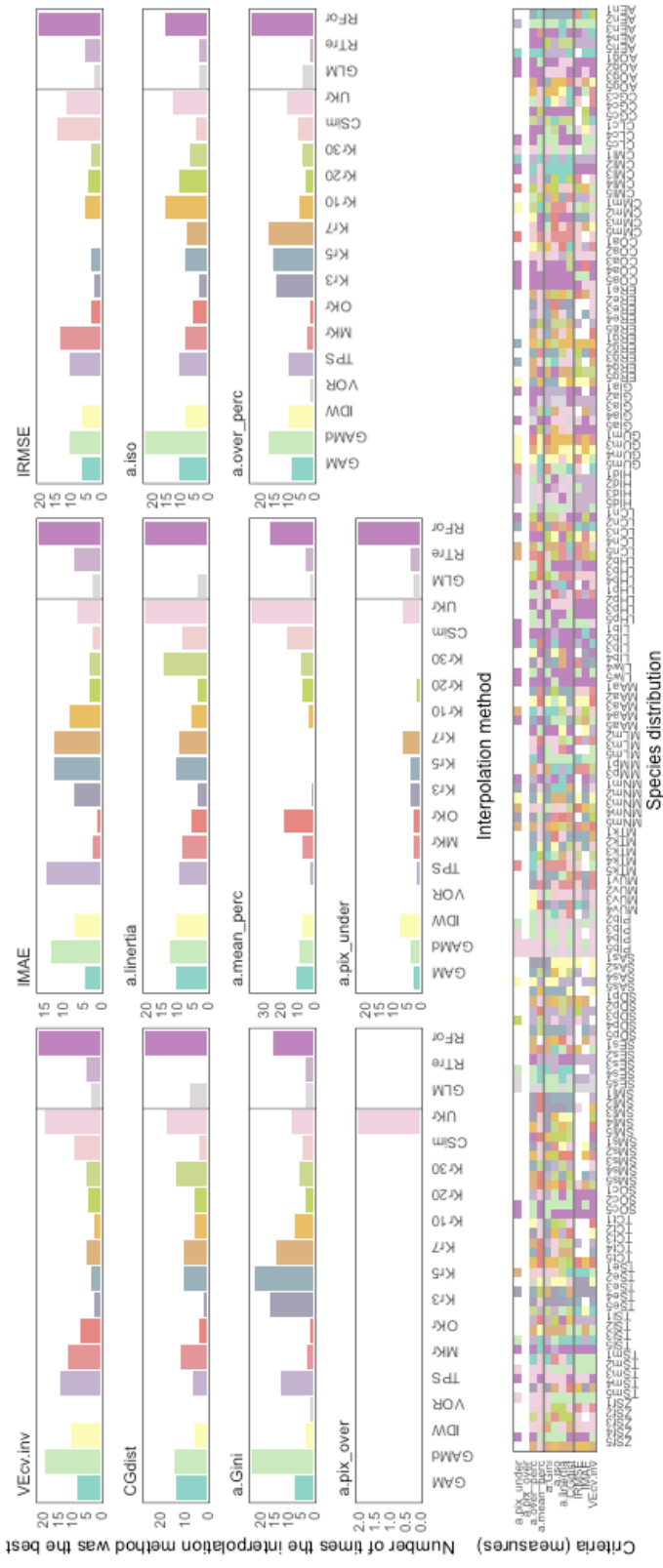
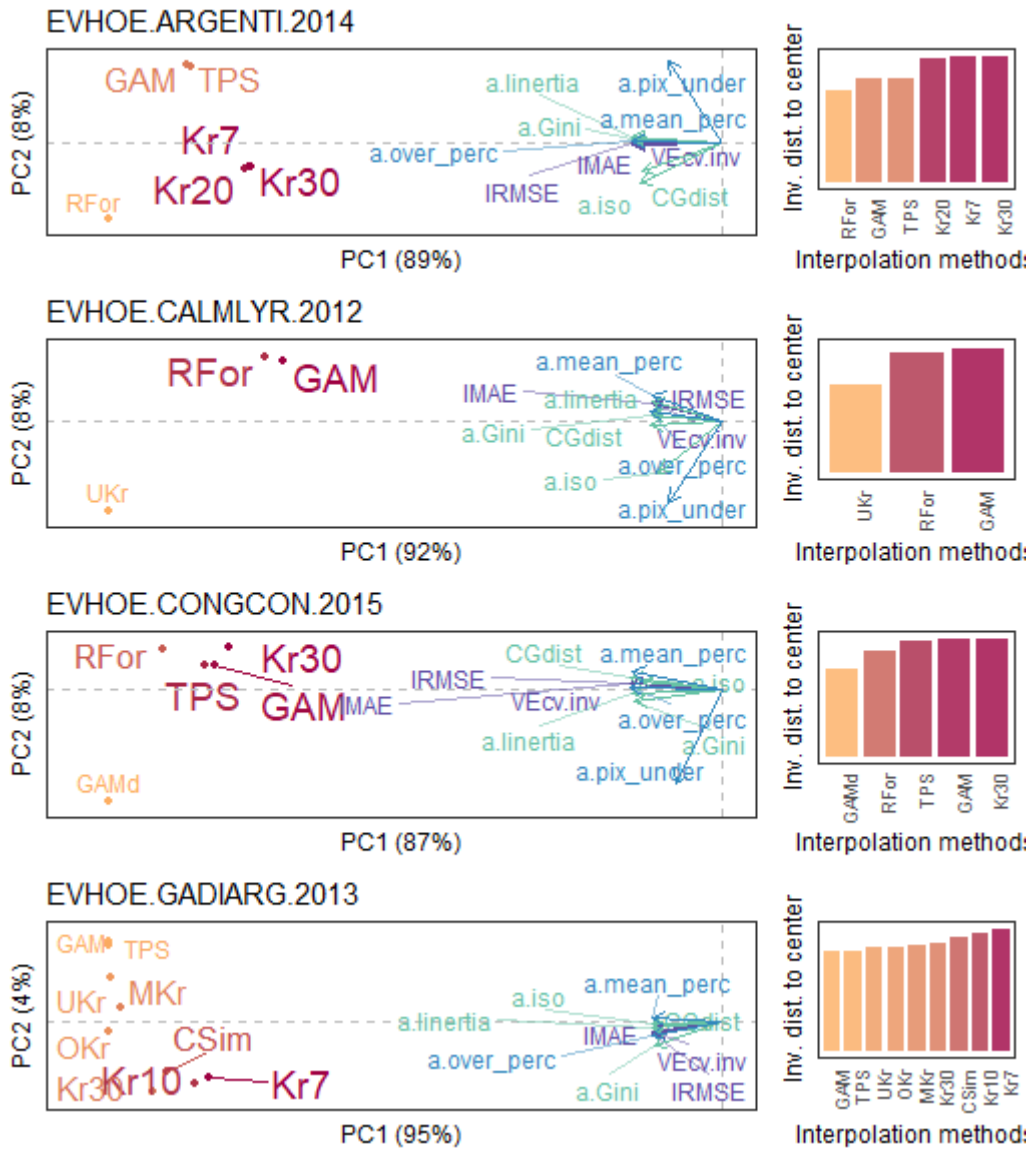
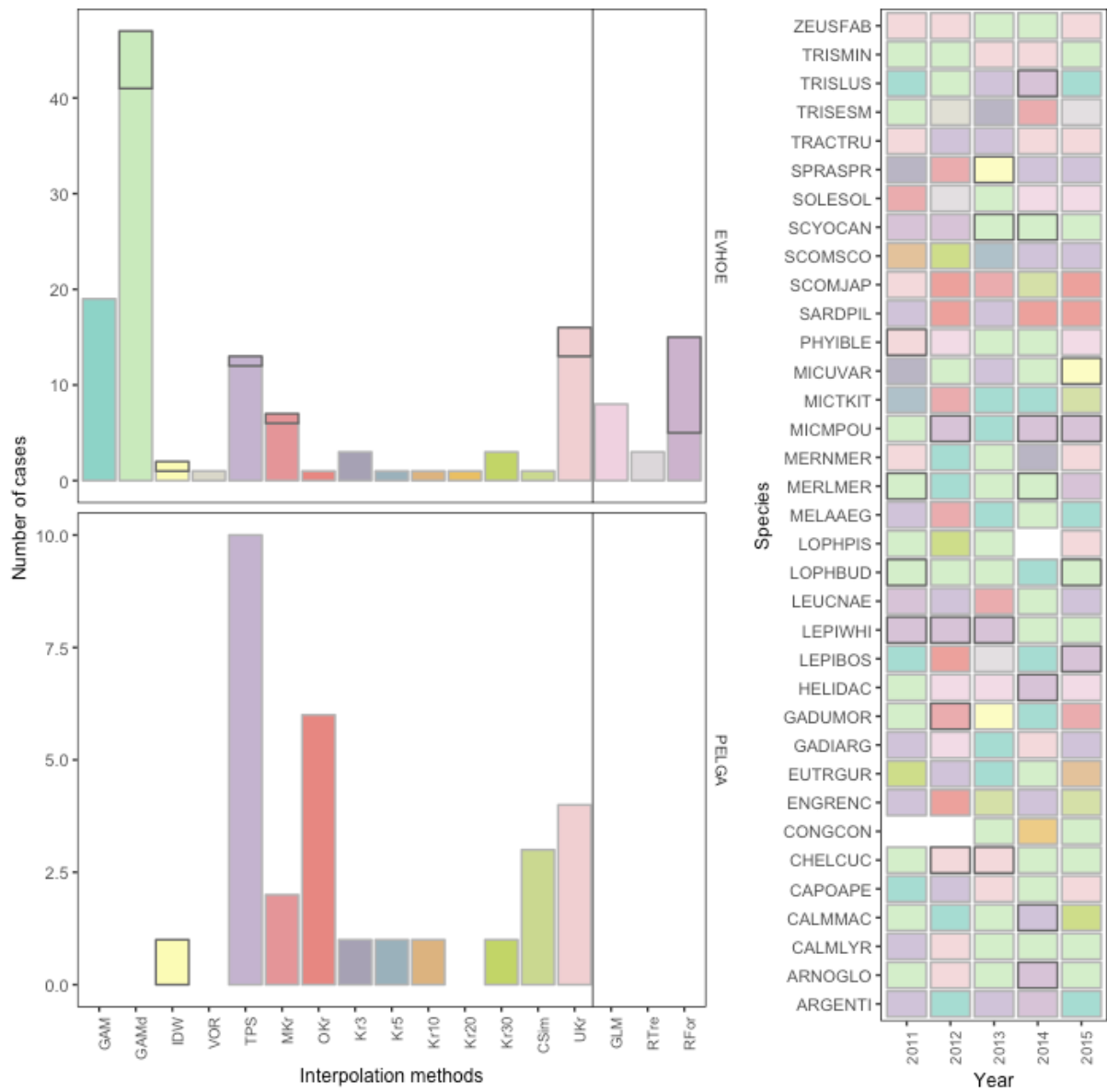


Fig. 7: second step PCA examples

page 1 of 1



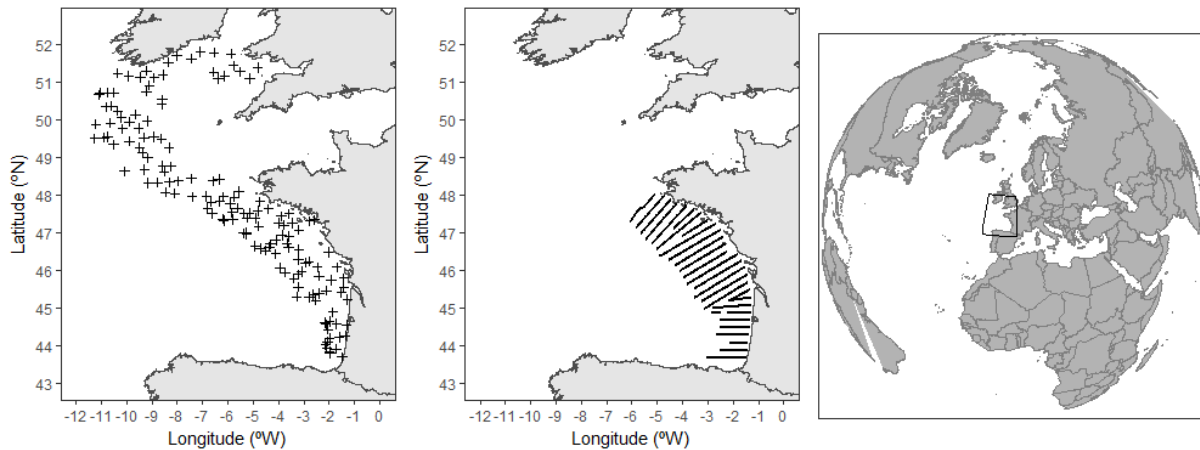
861 Fig. 8: Winning methods overall;



862  
863  
864  
865  
866

867 **Supplement 1**

868  
869 Location of the sampling stations from 2015 of the bottom trawl survey (EVHOE, left panel),  
870 of the pelagic acoustic survey (PELGAS) on the Gulf of Gascogne/Bay of Biscay in the North  
871 Atlantic coast of France (right panel). Number of hauls per year on EVHOE, from 2011 to 2015  
872 were respectively 220, 195, 208, 219 and 148.



873  
874 **Species list names and abbreviations**

875 EVHOE: *Argentina* sp. (ARGENTI), *Arnoglossus* sp. (ARNOGLO), *Callionymus lyra*  
876 (CALMLYR), *Callionymus maculatus* (CALMMAC), *Capros aper* (CAPOAPE),  
877 *Chelidonichthys cuculus* (CHELCUC), *Conger conger* (CONGCON), *Eutrigla gurnardus*  
878 (EUTRGUR), *Gadiculus argenteus* (GADIARG), *Gadus morhua* (GADUMOR), *Helicolenus*  
879 *dactylopterus* (HELIDAC), *Lepidorhombus boscii* (LEPIBOS), *Lepidorhombus whiffiagonis*  
880 (LEPIWHI), *Leucoraja naevus* (LEUCNAE), *Lophius budegassa* (LOPHBUD), *Lophius*  
881 *piscatorius* (LOPHPIS), *Melanogrammus aeglefinus* (MELAAEG), *Merluccius merluccius*  
882 (MERLMER), *Merlangius merlangus* (MERNMER), *Microchirus variegatus* (MICUVAR),  
883 *Micromesistius poutassou* (MICPOU), *Microstomus kitt* (MICKIT), *Phycis blennoides*  
884 (PHYIBLE), *Scyliorhinus canicula* (SCYOCAN), *Solea solea* (SOLESOL), *Trisopterus*  
885 *esmarkii* (TRISESM), *Trisopterus luscus* (TRISLUS), *Trisopterus minutus* (TRISMIN) and  
886 *Zeus faber* (ZEUSFAB)  
887 PELGAS: *Engraulis encrasicolus* (ENGRENC), *Sardina pilchardus* (SARDPIL), *Scomber*  
888 *japonicas* (SCOMJAP), *Scomber scombrus* (SCOMSCO), *Sprattus sprattus* (SPRASSPR) and  
889 *Trachurus trachurus* (TRACTRU)

890  
891 **Details of the survey:**

892 The EVHOE survey has been carried out on the R/V Thalassa, a stern trawler of 73.7 m length  
893 by 14.9 m wide (tonnage of 3022 t). The fishing gear used is a GOV 36/47 without exocet Kite  
894 which is replaced by 6 additional floats and with a horizontal opening of 20 m and a vertical  
895 opening of 4 m.

896 **Supplement 2**

897  
898 **Description of terrain variables:**

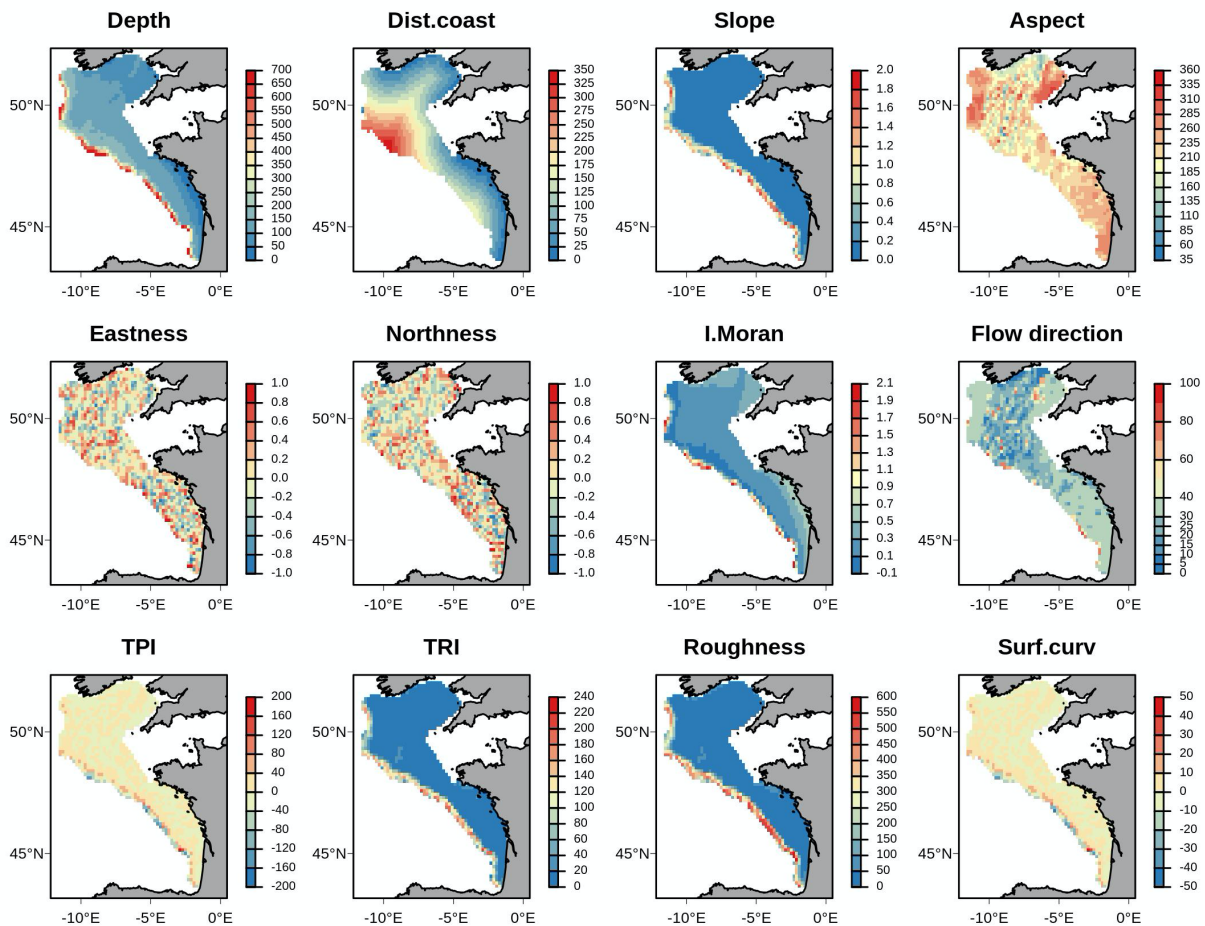
899 Slope represent the terrain steepness (arrangement and magnitude of elevation  
900 differences)(slope) whereas terrain aspect (aspect) measures its orientation in degrees, relative  
901 to the north and it is particularly important to exposure to currents or water movement (Wilson

902 et al., 2007). From aspect, northerness and easterness were derived (Wilson et al., 2007). Profile  
 903 curvature defines convex/concave areas, represented by the rate of slope change along a profile,  
 904 i.e. the surface of the steepest down-slope direction (surf.curv)(package ‘spatialEco’)(Evans JS,  
 905 2017). Bathymetric Position Index is the difference between the value of a cell and the mean  
 906 value of its surrounding cells and provides an indication of whether any particular pixel forms  
 907 part of a positive (e.g., crest) or negative a (e.g., trough) feature of the surrounding terrain (TPI,  
 908 marine version of the topographic position index). Terrain Ruggedness Index represents terrain  
 909 variability whereas roughness represents the bathymetric amplitude of a cell and its  
 910 surroundings (TRI). Surface flow confluence indicates the steepest downhill path (flowdir).  
 911 Local Moran I was calculated as a measure of local spatial autocorrelation in the bathymetric  
 912 neighborhood (moran)(Diesing et al., 2014; Li et al., 2016). Additionally, distance to the nearest  
 913 coast was also estimated (dist.coast).

914

915 **Maps of the topographic variables used in the current work (bottom trawl area, EVHOE)**

916 After gridding all variables to EVHOE prediction grid (1117 pixels, 15 km).



917

918

**Supplement 3**

919

920

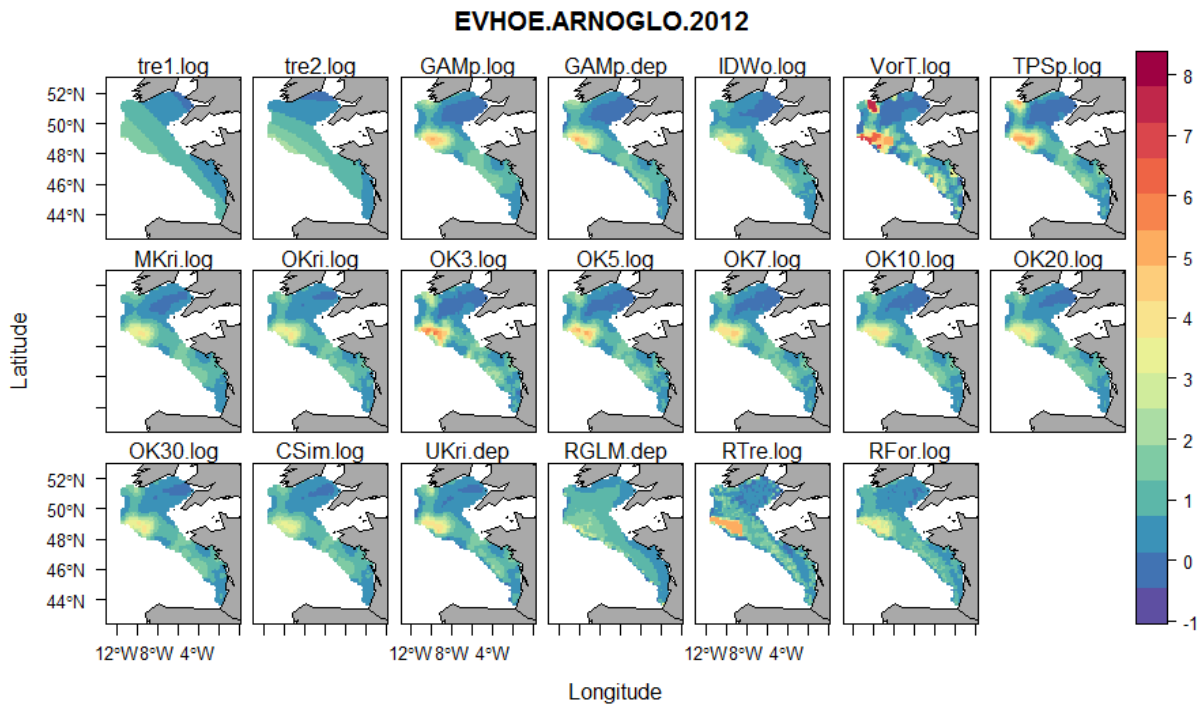
**Table 1: Summary of the interpolation methods used in the current work.**

Interpolator	Description	R-package /Function	Covar
<b>IMGeo</b>			
LM1	1st-order trend surface	gstat::gstat(vari ~ 1, degree=1)	-
LM2	2nd order trend surface	gstat::gstat(vari ~ 1, degree=2)	-
<b>GAM</b>	Generalized Additive Model		

	(Wood, 2006)		
GAM	GAM in function of lat and long (in UTM)	<code>mgcv ::gam (lvari ~ s(lat ,long))</code>	
GAMd	GAM in function of lat and long (in UTM) and depth	<code>mgcv ::gam (lvari ~ s(lat ,long)+s(Depth))</code>	Depth
IDW	Inverse distance weight		
IDW	Optimized using cross validation	<code>gstat::gstat(lvari~1, nmax=opt\$par[1], set=list(idp=opt\$par[2]))</code>	-
VOR	Voronoi tessellation (Fortin and Dale, 2005)	<code>dismo::voronoi(dat.s["lvari"])</code>	
TPS	Thin Plate Spline interpolation (Nychka, 2016)		
<b>Kriging</b>	Methods using kriging (Bivand et al., 2013)		
MKr	Ordinary kriging interpolation (manual fitting of variogram)	<code>gstat::krige(lvari ~ 1)</code>	-
CSim	Stochastic conditional simulation	<code>gstat::krige(lvari ~ 1, nsim = 1000, nmax = 20)</code>	-
OKri		<code>automap::autoKrige(lvari~1, model = c("Sph", "Exp"))(gstat)</code>	-
17-22. Kr3 Kr5 Kr7 Kr10 Kr20 Kr30 UKr	OK with various neighborhood	<code>automap::autoKrige(lvari~1, model = c("Sph", "Exp"), nmax=jj) (gstat)</code>	-
GLM	Multiple regression	<code>dat.s, lvari~Depth+slope+aspect+eastness+northness+surf.curv+TPI+TRI+rough+dist.coast+flowdir</code>	Depth +slope +aspect+east ness+northne ss+surf.curv +TPI+TRI+r ough+dist.co ast+flowdir
RTre	Regression tree	<code>rpart:: rpart ( dat.s, vari ~ Depth+slope+aspect+eastness+northness+surf.curv+TPI+TRI+rough+dist.coast+flowdir)</code>	Depth+slope +aspect+east ness+northne ss+surf.curv +TPI+TRI+r ough+dist.co ast+flowdir
RFor	Random forest	<code>randomForest: randomForest( dat.s, vari ~ Depth+slope+aspect+eastness+northness+surf.curv+TPI+TRI+rough+dist.coast+flowdir)</code>	Depth+slope +aspect+east ness+northne ss+surf.curv +TPI+TRI+r ough+dist.co ast+flowdir+ moran

921

922 Details on the spatial interpolation methods considered



923

924 **Methods using just geographic coordinates or depth (IMGeo)**

925 *1<sup>st</sup> and 2<sup>nd</sup> order trend surfaces (LM1 and LM2, respectively).*

926 In these interpolation methods, a first or second order trend surface is fitted to the raw data,  
 927 respectively. It is a simplistic approach that was included in the current work as a worst case  
 928 scenario that should be slightly better than a simple overall mean.

929 *Inverse distance weighting (IDW)*

930 Inverse distance weighting (IDW) is an advanced nearest neighbor approach that allows  
 931 including more observations than only the nearest points. The value at a certain grid cell is  
 932 obtained from a linear combination of the surrounding locations and the weight of each  
 933 observation is determined by the distance. IDW is an exact interpolator. The method is fast,  
 934 easy to implement and easily “tailored” for specific needs, but ancillary data cannot be  
 935 incorporated. The method tends to generate “bull’s eye patterns” (Sluiter, 2009).

936 *Voronoi tessellation (VorT)*

937 The nearest neighbors method predicts the value of an attribute at an unsampled point based on  
 938 the value of the nearest sample by drawing perpendicular bisectors between sampled points,  
 939 forming such as Voronoi polygons (or Dirichlet/ Thiessen). This produces one polygon per  
 940 sample and the sample is located in the center of the polygon, such that in each polygon all  
 941 points are nearer to its enclosed sample point than to any other sample points (Legendre and  
 942 Legendre, 1998; Li and Heap, 2008; Webster and Oliver, 2007). This technique is generally  
 943 used with point data or categorical variables, but can also be used with densities/biomasses  
 944 (Baddeley et al., 2006; Dauvin et al., 2004; Morfin et al., 2016; Thorson et al., 2015; Zuur et  
 945 al., 2007).

946 *Thin Plate Splines (TPS)*

947 Thin plate smoothing splines (TPS), formally known as “laplacian smoothing splines”. Similar  
 948 to the previous method, splines are fitted to the sampled data, but in this method, the smoothing  
 949 parameter is calculated by minimizing the generalized cross validation function (GCV). This

950 method is relatively robust because the minimization of GCV directly addresses the predictive  
951 accuracy and is less dependent on the veracity of the underlying statistical model (Hutchinson,  
952 1995) (Li and Heap, 2008). We applied this method using `package::fields`.

### 953 *Generalized Additive Models (GAM)*

954 Generalized additive models (GAM) are a semiparametric extension of generalized linear  
955 models (GLM), but allow nonlinear relationships between the response and explanatory  
956 variables (Wood, 2006), are very commonly used in biological studies (Guisan et al., 2002).  
957 GAMs have been often used as a method to produced spatial predictions (i.e. interpolation) by  
958 considering the geographic coordinates and its interaction as covariates (Augustin et al., 2013).  
959 In the current work we used a GAM applied with the geographic coordinates as covariates  
960 (`s(x,y, bs="ts")`)(GAM), a model where besides geographic coordinates, depth was also  
961 considered as covariate (GAMd). GAMs were applied using the `r` package `::mgcv` (Wood,  
962 2006).

### 963 *Kriging*

964 From an interpolation point of view, kriging is equivalent to a thin-plate spline and is one  
965 species among the many in the genus of weighted inverse distance methods, albeit with  
966 attractive properties. However, from a statistical point of view, kriging produces the “best linear  
967 unbiased prediction” for an unknown location. It is linear since the estimated values are  
968 weighted linear combinations of the available data, unbiased because the mean of the error is  
969 0, and it aims to minimize the variance of the errors (Cressie 1990). Several variations of kriging  
970 methods were selected following previous works, all applied in the log transformed data. A  
971 sequence of interpolation approaches was considered, starting with ordinary kriging with global  
972 mean (Okr using automatic modelling and Mkr using manual variogram fitting), ordinary  
973 kriging with local neighbourhood estimation (considering 3, 5, 7, 10, 20 and 30 neighbours.  
974 Kriging neighborhood is a defined area, in terms of shape and size. Only samples from this area  
975 are used in the computation of the local estimates using the kriging technique.

976 Kriging with external trend, also called universal kriging using depth as covariate (Ukr). It is  
977 an extension of OK by incorporating the local trend within the neighbourhood search widow as  
978 a smoothly varying function of the coordinates. UK estimates the trend components within each  
979 search neighbourhood window and then performs SK on the corresponding residuals.

### 980 *Stochastic conditional simulations (CSim)*

981 These techniques are used more and more, commonly to generate a series of spatial data that  
982 have a given degree of spatial dependence, in order to evaluate whether or not observed sample  
983 data show significant spatial patterns (Fortin and Dale, 2005). In this method, the parameters  
984 of the variogram model (defined previously for ordinary kriging) derived from the experimental  
985 variogram were used to generate 1000 stochastic simulations, with the same degree of spatial  
986 variance as the observed data (Fortin and Dale, 2005). These methods are known to generate  
987 maps having more spatial variability than the kriged ones and hence looking more realistic in  
988 comparison to the observed map (Fortin and Dale, 2005).

### 989 **Methods using topographic covariates (IMCov)**

990 In a mixed method approach to interpolation, the final predictions result of a combination of  
991 methods. The main trends are modelled in function of a group of selected covariates in first step  
992 (for example General Linear Model (GLM) or machine learning). In a second step, the residuals  
993 of this model are then analyzed using kriging, and then incorporated into the predictions (Hengl  
994 et al., 2007, 2004; Li et al., 2016). These methods require the availability of covariates. In the  
995 current work we used the marine topographic variables derived from GEBCO bathymetric  
996 maps, therefore widely available at a worldwide scale. Three mixed models were considered,  
997 one using general linear model and two using machine learning algorithms, regression trees and  
998 random forest.

### 999 *Multiple regression (GLM)*



1000 Stepwise multiple regression with all topography-depth covariates was carried out for each  
 1001 distribution ( $lvari \sim \text{Depth} + \text{slope} + \text{rough} + \text{moran} + \text{TRI} + \text{TPI} + \text{dist.coast} + \text{flowdir} + \text{aspect}$   
 1002  $+ \text{eastness} + \text{northness}$ ). The regression model considered assumes that the residuals are  
 1003 generated from a normally distributed, second-order stationarity random process—i.e. a random  
 1004 process that has a constant mean and variance.

1005 *Regression trees (RTre)*

1006 The regression tree approach (also known as binary decision trees) uses binary recursive  
 1007 partitioning whereby the data of the primary variable are successively split along the gradient  
 1008 of the explanatory variables into two descendent subsets or nodes. These splits occur so that at  
 1009 any node the split is selected to maximize the difference between two split groups or branches.  
 1010 The mean value of the primary variable in each terminal node can then be used to map the  
 1011 variable across the region of interest (Li and Heap, 2008). Regression tree (CART) algorithm  
 1012 was fitted to the data to produce a tree with optimal tree size.

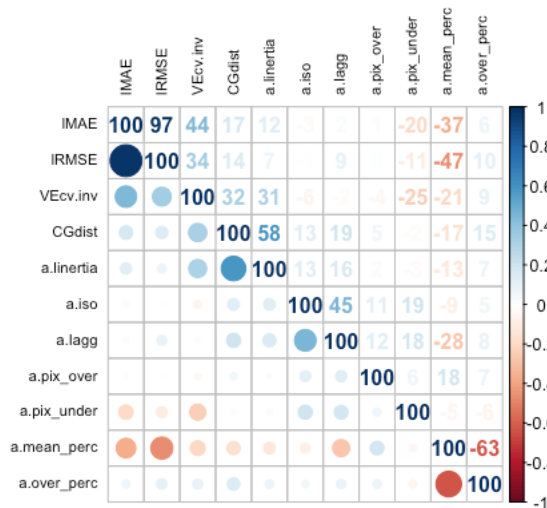
1013 *Random forest (RFor)*

1014 A random forest model of each species distribution in function of all marine topographic  
 1015 covariates was produced (Hengl et al., 2015; Li et al., 2016, 2013, 2011)( $vari \sim \text{Depth} + \text{slope}$   
 1016  $+ \text{aspect} + \text{eastness} + \text{northness} + \text{surf.curv} + \text{TPI} + \text{TRI} + \text{rough} + \text{moran} + \text{dist.coast} + \text{flowdir}$ ).  
 1017  
 1018

1019 **Supplement 4**

1020

1021 Correlation plot between the indicators



1022

1023 **Supplement 5**

1024

1025

1026 # title: "Example script for the selection of interpolation method"

1027 # author: "Marta M Rufino^[EMH, IFREMER]"

1028

1029 # The aim of this script is to provide an example of the selection of an interpolation method.

1030 This is an accompanying work of the paper.

```

1031
1032 # We will need to have these packages intalled:
1033 require(ggplot2); require(RColorBrewer); require(gridExtra) # plotting
1034 require(dplyr); require(tidyr);#data manipulation
1035 require(raster); require(rasterVis); #plot and spatial data manipulation
1036 require(sp); # spatial data
1037 require(gstat); #kriging and idw
1038 require(fields) #tps
1039 require(mgcv); #gam
1040 require(RGeostats) #spatial indicators. Pkg can be download from here
1041 http://rgeostats.free.fr/download.php and install manually
1042 require(ineq) #Gini index (spatial indicators)
1043 require(ggplot) # PCA plot
1044
1045 # Get an example running with MEUSE dataset:
1046 library(sp); library(gstat)
1047 data(meuse)
1048 data(meuse.grid)
1049 gridded(meuse.grid) = ~x+y
1050 # m <- vgm(.59, "Sph", 874, .04)
1051
1052 dat = meuse %>%
1053   dplyr::select(x,y,zinc, dist) %>%
1054   dplyr::rename("vari" = "zinc",
1055     "Depth" = "dist")
1056 dat.grid <- meuse.grid["dist"]
1057 names(dat.grid) = "Depth"
1058
1059 # 1. Interpolate the data (function interp.dat_CV)
1060
1061 # First we make the different spatial interpolation models. For each model, we will do cross
1062 validation. We will only consider the models without covariates to facilitate the process.
1063
1064 ## This chunk runs a function to interpolate the data of each species distribution
1065 (interp.dat_CV) and estimate respective CV
1066
1067 ## DataDir should be the directory where you have your functions file
1068 ('interp.dat_CV_script.r')
1069
1070 # Please run the required functions which are in the end of the script
1071
1072 # Run the function
1073 kk <- interp.dat_CV(nam="zinc", dat=dat, dat.grid=dat.grid, CV=TRUE, plotit=FALSE,
1074   replicate.cv = 10)
1075 # note we only used 10 replicates of the cv instead of 100 to make a quicker test
1076
1077 # see the results:
1078 head(kk)
1079 # the result of this function is a list with three items:
1080 # 1. res is the raster stack with all predictions from each method;

```

```

1081 # 2. cv.results is the cross-validation summary results
1082 # 3. model.params is some of the models parameters stored
1083
1084 # Extract the raster stack with all interpolator predictions and store it as a new object
1085 pred = kk$res
1086 names(pred)
1087
1088 # Plot the interpolations
1089 coli <- function (region = rev(brewer.pal(n = 10, 'Spectral')), ...)
1090 {theme <- rasterTheme(region = region, ...); theme}
1091 levelplot(pred, par.settings = coli)
1092
1093 # Reshape the table to fit nicely in the results
1094 cv.res <- left_join(
1095   data.frame(kk$cv.results) %>%
1096   dplyr::select(Index, median, method) %>%
1097   tidyr::spread(Index, median),
1098   data.frame(kk$cv.results) %>%
1099   dplyr::filter(Index=="VEcv") %>%
1100   dplyr::select(VEcv.Q1, VEc.v.Q3, method) )
1101
1102 # Reorder factor levels
1103 cv.res$method <- factor(cv.res$method,
1104   levels=c("tre2", "GAMp", "IDWo",
1105     "TPSp", "MKri", "UKri"))
1106
1107 # Round
1108 cv.res[,-c(1)] <- round(cv.res[,-c(1)],2)
1109
1110 # Make the log of the measures
1111 cv.res$MAE <- log1p(cv.res$MAE)
1112 cv.res$RMSE <- log1p(cv.res$RMSE)
1113
1114 # Classify VEc.v
1115 cv.res$VEcv.class <- cv.res$VEcv
1116 cv.res$VEcv.class <- cut(cv.res$VEcv.class, c(-2,0,10, 30, 50, 80, 100))
1117 levels(cv.res$VEcv.class) <-
1118   c("0. worst_then_mean",
1119     "1.very_poor",
1120     "2.poor",
1121     "3.average",
1122     "4.good",
1123     "5.excellent")
1124
1125 # Inverted VEc.v, i.e. the bigger the worst:
1126 cv.res$VEcv.inv <- abs(cv.res$VEcv/100-1)*100
1127
1128 # Estimate spatial indicators
1129

```

```

1130 # In this chunk we will estimate the spatial indicators using the sampled data and the
1131 interpolated data (prediction rasters).
1132
1133 # For this we will use the pre-packed functions in the packages 'Rgeostats' and 'ineq', although
1134 the indexes are relatively simple to calculate.
1135
1136 # Further, the function will also estimate the 'data limits integrity indicators'.
1137
1138 # This chunk estimates the difference in the spatial indicators between the raw data and
1139 interpolated surfaces and the data limits integrity indicators
1140
1141 # Note we require RGeostats and ineq for this chunk.
1142
1143 # Test the function in one case
1144 fun.inter2(ii="tre2", dat=dat, pred=pred)
1145
1146 # Apply to all interpolation methods:
1147 ind.res <- lapply(as.list(levels(cv.res$method)), fun.inter2, dat=dat, pred=pred)
1148 ind.res <- do.call("bind_rows", ind.res)
1149
1150 # Merge the results with cv results:
1151 tot.res <- full_join(cv.res, ind.res, by=c("method"))
1152
1153 # Now, all the indicators were estimated for each interpolation method. We shall then proceed
1154 to make the first step of the selection method.
1155
1156 # First selection step: VEcv interquantile range
1157
1158 # Reorder factor levels:
1159 tot.res$method <- factor(tot.res$method,
1160                       levels=c("tre2", "GAMp", "IDWo",
1161                                "TPSp", "MKri", "UKri"))
1162 tot.res$short.method <- ordered(tot.res$method,
1163                               labels=c("LM2", "GAM", "IDW", "TPS", "MKr", "UKr"))
1164
1165
1166 # Which methods have the VEcv higher than the lower Q3
1167 tot.res <- tot.res %>%
1168   dplyr::select(-MAE, -R2, -RMSE) %>%
1169   # valid methods, i.e. within range of inter-quartile:
1170   dplyr::mutate(
1171     VEcv.criteria = c(VEcv.Q3 >= max(VEcv.Q1)))
1172
1173 # Plot the VEcv, Q1 and Q3 and respective criteria
1174 tot.res %>%
1175   ggplot(aes(x=method, y=VEcv))+
1176   geom_point(aes(col=VEcv.criteria))+
1177   geom_crossbar(aes(ymin=VEcv.Q1, ymax=VEcv.Q3, y=VEcv, col=VEcv.criteria), alpha=.5,
1178               width=.5)+
1179   ggtitle("First step of interpolators selection")

```

```

1180
1181
1182 # Second selection step: indicators
1183
1184 # select the data for the PCA of indicators
1185 row.names(tot.res) = tot.res$short.method
1186 sec.res <- tot.res %>%
1187   dplyr::filter(VEcv.criteria==TRUE) %>%
1188   dplyr::select(VEcv.inv, LMAE, LRMSE,
1189               CGdist, a.linertia, a.iso, a.Gini,
1190               a.pix_under, a.pix_over, a.mean_perc, a.over_perc)
1191
1192 # Use the function to plot the results and estimate the best method of the selection
1193 PCbiplot(datpc=sec.res, x="PC1", y="PC2")
1194
1195
1196
1197 #####
1198 ## Functions required
1199 #####
1200
1201
1202
1203 interp.dat_CV <- function(nam, dat, dat.grid,
1204                          CV=TRUE, plotit=TRUE,
1205                          replicate.cv = 10){
1206   require(ggplot2); require(RColorBrewer); # plotting
1207   require(dplyr); require(tidyr);#ploting and manover
1208   require(raster); require(rasterVis); #plot and manipulation
1209   require(sp); # spatial data
1210   require(gstat); #kriging and idw
1211   require(fields) #tps
1212   require(mgcv); #gam
1213   #require(scales) #modeling
1214   theme_set(theme_bw(base_size = 9));
1215
1216   # Arguments:
1217   # nam is the label code
1218   # dat data frame with x, y, vari (variable of interest) and Depth
1219   # dat.grid # predictions grid that we want to estimate. class SpatialPixels - sp
1220   # plotit: produce plots for each interpolation.
1221
1222   # Start the function
1223
1224   # make a raster stack to fill with interpolation predictions of the different models:
1225   dat.pred <- raster(dat.grid)
1226   dat.pred[] <- NA
1227   dat.pred <- stack(dat.pred)
1228   # make a dataframe to fit in the parameters
1229   model.params <- data.frame(code=as.character(nam))

```

```

1230
1231 ## make the spatial object
1232 dat.s <- dat
1233 coordinates(dat.s) <- ~x+y
1234 # the warning is due to the recent change to PROJ6
1235 proj4string(dat.s) <- CRS("+init=epsg:28992")
1236 proj4string(dat.grid) <- CRS("+init=epsg:28992")
1237 #dat.border <- spTransform(dat.border, utm30)
1238 #dat.pred <- stack(raster(dat.grid)) # obj to save the data
1239
1240 # for plotting
1241 coli <- function (region = rev(brewer.pal(n = 10, 'Spectral')), ...)
1242 {theme <- rasterTheme(region = region, ...); theme}
1243
1244 # function to make individual plots
1245 fun.plot <- function(ii, dat.s){
1246   print(levelplot(dat.pred[[ii]]+.1, main=paste(ii, nam, round(max(dat$vari))),
1247     zscaleLog=FALSE,
1248     par.settings = coli))}
1249
1250 # Function to estimate error measures
1251 fun.eval <- function(observed, predicted){
1252   resi <- c(observed- predicted)
1253   # rmse(sim=predicted, obs=observed)
1254   (RMSE <- sqrt(mean(resi^2)))
1255   #mae(sim=predicted, obs=observed)
1256   (MAE <- mean(abs(resi)))
1257   #(RMAE = MAE/mean(observed))
1258   #RMAE2 = mean(abs((kk$predicted-kk$observed)/mean(kk$observed)))*100
1259   #(RRMSE = RMSE/mean(observed))
1260   #RRMSE2 = sqrt(mean((kk$predicted-kk$observed)/mean(kk$observed)^2))*100
1261   # R2 should be 1-sum((kk$observed-kk$predicted)^2)/sum((kk$observed-
1262   mean(kk$observed))^2)
1263   (R2 <- 1-(sum((resi)^2)/sum((observed-mean(observed))^2)))
1264   #1-(RMSE/sqrt(mean((kk$observed-mean(kk$observed))^2))))
1265   #(R3 <- 1-var(resi)/var(kk$observed)) #HENGL
1266   (VEcv <- (1 - sum((resi)^2)/
1267     sum((observed-mean(observed))^2))*100)
1268   res.error <- data.frame(RMSE=round(RMSE,2),
1269     MAE=round(MAE,2),
1270     #RMAE=round(RMAE,2), RRMSE=round(RRMSE,2),
1271     R2=round(R2,2),
1272     VEcv=round(VEcv,2))
1273   return(res.error)
1274 }
1275
1276 # Function to make the cross validation and estimate error measures
1277 cvfun.replicate <- function(xx, FUN, ii=ii, nam=nam, replicate.cv=replicate.cv){
1278   # xx is the data frame with x,y and biom..., FUN is the fun model of each method;
1279   # xx=dat.s; FUN=cv1.fun.cv; replicate.cv=10

```

```

1280 cv2.fun.fold <-function(xx, FUN){
1281   set.seed(seed <- as.integer(runif(1)*2e9))
1282   print(seed)
1283   kf <- sample(rep(seq_len(10), length.out=nrow(dat)))
1284   # Apply fun for the 10 folds
1285   kk <- lapply(as.list(sort(unique(kf))),
1286               FUN = FUN, xx=xx, kf=kf) %>%
1287     dplyr::bind_rows()
1288   kk$seed=seed
1289   ## if we want to export predicted/observed
1290   #write.table(kk, append=TRUE,
1291               #   file = paste0(paste("pred.obs_cv1000", nam, ii, sep="_"), ".xls"),
1292               #   sep="\t", row.names=FALSE, col.names=FALSE)
1293   assign("last.warning", NULL, envir = baseenv())
1294
1295   kk <- kk %>%
1296     dplyr::group_by(fold) %>%
1297     do(fun.eval(observed=.$observed, predicted=.$predicted)) %>%
1298     dplyr::filter(is.finite(VEcv)) %>%
1299     ungroup() %>%
1300     dplyr::summarise_all(funs(mean)) %>%
1301     dplyr::select(RMSE:VEcv) %>%
1302     data.frame()
1303   return(kk)
1304   rm(kf, kk, seed)
1305 }
1306
1307 # to test cv2.fun.fold(FUN = cv1.fun.cv, xx=dat)
1308 # replicate CV 100 times
1309 xx1 <- replicate(replicate.cv, cv2.fun.fold(FUN = FUN, xx=xx), simplify = FALSE) %>%
1310   bind_rows %>%
1311   mutate(sp=nam, method=ii)
1312 xx1[mapply(is.infinite, xx1)] <- NA
1313 xx1 <- na.exclude(xx1)
1314 ## plot the distribution
1315 #print(xx1 %>% tidyr::gather(Index, value, RMSE:VEcv) %>%
1316 #   ggplot(aes(x=value, group=Index, col=Index))+geom_density()+facet_wrap(~Index,
1317 scales="free"))
1318 ## if we want to export the results:
1319 # write.table(xx1, file = paste("indices_cv1000", nam, ii, ".xls", sep="_"), sep="\t",
1320 row.names=FALSE)
1321
1322 # Get stats
1323 kk1 <- xx1 %>% tidyr::gather(Index, value, RMSE:VEcv) %>%
1324   dplyr::group_by(Index) %>%
1325   dplyr::summarize(VEcv.Q1=quantile (value, probs=0.25),
1326                   VEcv.Q3=quantile(value, probs=0.75),
1327                   mean=mean(value, na.rm=TRUE), N=n(),
1328                   median=median(value, na.rm=TRUE), N=n(),
1329                   max=max(value, na.rm=TRUE),

```

```

1330         min=min(value, na.rm=TRUE)) %>%
1331     dplyr::mutate(sp=nam, method=ii)
1332     return(kk1); rm(xx)
1333 }
1334
1335
1336 #####
1337 # 2nd order trend surface
1338 #####
1339 ii <- "tre2"
1340 dat.trend2 <- gstat(formula=vari ~ 1, data=dat.s, degree=2)
1341 dat.trend2 <- predict(dat.trend2, newdata=dat.grid)
1342 #spplot(dat.trend2[1], contour=TRUE,main="2nd order trend surface interpolation")
1343 dat.pred[[ii]] <- raster(dat.trend2[1])
1344
1345 # Cross validation replicate
1346 if(CV==TRUE){
1347     # function to do CV on each fold
1348     cv1.fun.cv = function(xx, k, kf){
1349         # Function to reproduce the interpolator
1350         # for a part of the data and predict with the other part
1351         # the output MUST be a dataframe with:
1352         # fold/observed/predicted
1353         kk <- gstat(formula=vari ~ 1, data=xx[kf != k,], degree=2)
1354         kk1 <- predict(kk, newdata=xx[kf == k,])
1355         return(data.frame(fold = k, observed = xx[kf == k,]$vari,
1356             predicted = kk1$var1.pred))
1357     }
1358     rm(kk, kk1, k)
1359     kk <- cvfun.replicate(xx=dat.s, FUN=cv1.fun.cv, ii=ii, nam=nam, replicate.cv=replicate.cv)
1360     cv.results <- kk;
1361 }
1362
1363
1364 #####
1365 ## GAM model
1366 #####
1367 require(mgcv)
1368 ii="GAMp"
1369 dat.mod <- gam(vari~s(x,y, bs="ts"), data=dat)
1370 kk <- data.frame(coordinates(dat.grid));
1371 names(kk)= c("x","y")
1372 dat.mod2 <- predict(dat.mod, newdata=kk)
1373 kk <- cbind(kk, dat.mod2)
1374 dat.pred[[ii]] <- rasterFromXYZ(kk)
1375 # store parameters
1376 model.params$R2.GAMp <- summary(dat.mod)$r.sq
1377
1378 # Cross validation replicate
1379 if(CV==TRUE){

```



```

1380 # function to do CV on each fold
1381 cv1.fun.cv = function(xx, k, kf){
1382   kk <- gam(vari ~ s(x,y, bs="ts", k=50), data=xx[kf != k,])
1383   kk1 <- predict(kk, newdata=xx[kf == k,])
1384   return(data.frame(fold=k, observed=xx[kf == k,]$vari,
1385     predicted=kk1))
1386   # kk <- gam(vari ~ s(x, y, bs="ts", k=50), data=xx[kf != k,])
1387   # #print(summary(kk)); print(plot(kk))
1388   # kk1 <- predict(kk, newdata=xx[kf == k,])
1389   # return(data.frame(fold=k, observed=xx[kf == k,]$vari, predicted=kk1))
1390   rm(kk, kk1, k)
1391 }
1392 # test: cv1.fun.cv(xx=dat, k=1, kf=kf)
1393 kk <- cvfun.replicate(xx=dat, FUN=cv1.fun.cv, ii=ii, nam=nam, replicate.cv=replicate.cv)
1394 print(head(kk))
1395 cv.results <- bind_rows(cv.results, kk);
1396 rm(kk)
1397 }
1398
1399 rm(dat.mod, dat.mod2, ii)
1400
1401
1402 # #####
1403 # # Inverse distance weighting interpolation OPTIMIZED
1404 # #####
1405 ii="IDWo"
1406 RMSE <- function(observed, predicted) {
1407   sqrt(mean((predicted - observed)^2, na.rm=TRUE))}
1408
1409 f1 <- function(x, test, train) {
1410   nmX <- x[1]
1411   idp <- x[2]
1412   if (nmX < 1) return(Inf)
1413   if (idp < .001) return(Inf)
1414   m <- gstat(formula=vari~1, locations=train, nmax=nmX, set=list(idp=idp))
1415   p <- predict(m, newdata=test, debug.level=0)$var1.pred
1416   RMSE(test$vari, p)
1417 }
1418 # set.seed(20150518)
1419 i <- sample(nrow(dat.s), 0.2 * nrow(dat.s))
1420 tst <- dat.s[i,]
1421 trn <- dat.s[-i,]
1422 opt <- optim(c(8, .5), f1, test=tst, train=trn)
1423
1424 dat.idwopt <- gstat(formula=vari~1, locations=dat.s, nmax=opt$par[1],
1425 set=list(idp=opt$par[2]))
1426 dat.idwopt <- raster::interpolate(raster(dat.grid), dat.idwopt)
1427 ## [inverse distance weighted interpolation]
1428 dat.idwopt <- mask(dat.idwopt, dat.grid)
1429 dat.pred[[ii]] <- dat.idwopt

```

```

1430
1431 # Cross validation replicate
1432 if(CV==TRUE){
1433   # function to do CV on each fold
1434   cv1.fun.cv = function(xx, k, kf){
1435     kk <- gstat(formula=vari~1, locations=xx[kf != k,], nmax=opt$par[1],
1436 set=list(idp=opt$par[2]))
1437     kk1 <- predict(kk, newdata=xx[kf == k,])
1438     return(data.frame(fold=k, observed=xx[kf == k,]$vari,
1439 predicted=kk1$var1.pred))
1440     rm(kk, kk1, k)
1441   }
1442   # test: cv1.fun.cv(xx=dat.s, k=1, kf=kf)
1443   kk <- cvfun.replicate(xx=dat.s, FUN=cv1.fun.cv, ii=ii, nam=nam, replicate.cv=replicate.cv)
1444   print(head(kk))
1445   cv.results <- bind_rows(cv.results, kk); rm(kk)
1446 }
1447 rm(i,tst, trn, opt,fl)
1448
1449
1450 #####
1451 # TPS
1452 #####
1453 print(ii <- "TPSp")
1454 kk <- Tps(coordinates(dat.s), dat.s$vari)
1455 dat.tps <- raster::interpolate(raster(dat.grid), kk)
1456 dat.tps <- mask(dat.tps, dat.grid)
1457 dat.pred[[ii]] <- dat.tps
1458
1459 # Cross validation replicate
1460 if(CV==TRUE){
1461   # function to do CV on each fold
1462   cv1.fun.cv = function(xx, k, kf){
1463     kk <- Tps(coordinates(xx[kf != k,]), xx[kf != k,]$vari)
1464     kk1 <- predict(kk, coordinates(xx[kf == k,]))
1465     return(data.frame(fold=k, observed=xx[kf == k,]$vari,
1466 predicted=c(kk1)))
1467     rm(kk, kk1, k)
1468   }
1469   # test: cv1.fun.cv(xx=dat.s, k=1, kf=kf)
1470   kk <- cvfun.replicate(xx=dat.s, FUN=cv1.fun.cv, ii=ii, nam=nam, replicate.cv=replicate.cv)
1471   print(head(kk))
1472   cv.results <- bind_rows(cv.results, kk); rm(kk)
1473 }
1474
1475
1476 #####
1477 # Manual kriging
1478 #####
1479 print(ii <- "MKri")

```

```

1480 dat.vgm <- variogram(vari~1, dat.s)
1481
1482 kk = vgm(psill = max(dat.vgm$gamma), model="Sph", range=max(dat.vgm$dist)/2,
1483 nugget=min(dat.vgm$gamma))
1484 dat.fit <- fit.variogram(dat.vgm, model = kk)
1485 ## plot variogram with respective model
1486 #plot(dat.vgm, dat.fit)
1487
1488 dat.krige <- krige(vari ~ 1, dat.s, dat.grid, model = dat.fit)
1489 #spplot(dat.krige[1])
1490 dat.pred[[ii]] <- raster(dat.krige[1])
1491 model.params <- cbind(model.params, "MKri"=data.frame(nug=dat.fit[1,2], sill=dat.fit[2,2],
1492 range=dat.fit[2,3]))
1493
1494 # Cross validation replicate
1495 if(CV==TRUE){
1496 # function to do CV on each fold
1497 cv1.fun.cv = function(xx, k, kf){
1498   kk <- krige(vari ~ 1, xx[kf != k,], xx[kf == k,], model = dat.fit)
1499   return(data.frame(fold=k, observed=xx[kf == k,]$vari,
1500     predicted=kk$var1.pred))
1501   rm(kk, kk1, k)
1502 }
1503 # test: cv1.fun.cv(xx=dat.s, k=1, kf=kf)
1504 kk <- cvfun.replicate(xx=dat.s, FUN=cv1.fun.cv, ii=ii, nam=nam, replicate.cv=replicate.cv)
1505 print(head(kk))
1506 cv.results <- bind_rows(cv.results, kk);
1507 rm(kk)
1508 }
1509
1510
1511 #####
1512 # Universal kriging
1513 #####
1514 print(ii <- "UKri")
1515 dat.vgm <- variogram(vari~Depth, dat.s)
1516
1517 kk = vgm(psill = max(dat.vgm$gamma), model="Sph", range=max(dat.vgm$dist)/2,
1518 nugget=min(dat.vgm$gamma))
1519 dat.fit <- fit.variogram(dat.vgm, model = kk)
1520 #plot(dat.vgm, dat.fit)
1521
1522 dat.krige <- krige(vari ~ 1, dat.s, dat.grid, model = dat.fit)
1523 #spplot(dat.krige[1])
1524 dat.pred[[ii]] <- raster(dat.krige[1])
1525 model.params <- cbind(model.params, "UKri"=data.frame(nug=dat.fit[1,2], sill=dat.fit[2,2],
1526 range=dat.fit[2,3]))
1527
1528 # Cross validation replicate
1529 if(CV==TRUE){

```

```

1530 # function to do CV on each fold
1531 cv1.fun.cv = function(xx, k, kf){
1532   kk <- krige(vari ~ Depth, xx[kf != k,], xx[kf == k,], model = dat.fit)
1533   return(data.frame(fold=k, observed=xx[kf == k,]$vari,
1534     predicted=kk$var1.pred))
1535   rm(kk, kk1, k)
1536 }
1537 # test: cv1.fun.cv(xx=dat.s, k=1, kf=kf)
1538 kk <- cvfun.replicate(xx=dat.s, FUN=cv1.fun.cv, ii=ii, nam=nam, replicate.cv=replicate.cv)
1539 print(head(kk))
1540 cv.results <- bind_rows(cv.results, kk);
1541 rm(kk)
1542 }
1543
1544
1545 #####
1546 ## FINAL PLOTS
1547 #####
1548
1549 ## exclude Depth layer and project if wanted
1550 # res <- projectRaster(dat.pred, crs=myCRS)
1551 res = stack(dat.pred[[-1]])
1552
1553 if(plotit == TRUE){
1554   par(ask=TRUE)
1555   #samples
1556   p1<- qplot(data=dat, x=x, y=y, size=vari, col=vari, alpha=.0)+
1557     ggtitle(paste(nam,
1558       "max:", round(max(dat$vari)),
1559       "mean:", round(mean(dat$vari))))
1560
1561   # maps
1562   p2 <- levelplot(res,
1563     main=paste(nam, round(max(dat$vari))),
1564     zscaleLog=FALSE,layout=c(6, 1),
1565     par.settings = coli)
1566
1567   # log maps
1568   p3 <- levelplot(res+.1, main="Log", zscaleLog=TRUE,
1569     layout=c(6, 1),par.settings = coli)
1570   # scaled maps
1571   p4 <- levelplot(scale(res), main=paste('Scaled', nam),
1572     layout=c(6, 1),par.settings = coli)
1573
1574   # histogram
1575   p5 <- histogram(res,
1576     xlim=c(0,max(dat$vari)))
1577   # density
1578   p6 <- densityplot(res,
1579     xlim=c(0,max(dat$vari)))

```

```

1580
1581 # boxplot
1582 p7 <- bwplot(res)
1583
1584 grid.draw(grid.arrange(p2,p3,p4,
1585                       layout_matrix = rbind(c(1,1,1),c(2,2,2),c(3,3,3))))
1586 grid.draw(grid.arrange(p5,p1,p6,p7,
1587                       layout_matrix = rbind(c(1,1,1),c(2,3,4))))
1588 par(ask=FALSE)
1589 }
1590
1591 return(list(res = res,
1592           cv.results = cv.results,
1593           model.params = model.params))
1594
1595 assign("last.warning", NULL, envir = baseenv())
1596 # res <- tidy::gather(data.frame(res), method, pred, -x,-y)
1597 }
1598
1599 # to test
1600 # kk <- interp.dat_CV(nam="zinc", dat=dat, dat.grid=dat.grid, CV=TRUE, plotit=TRUE)
1601
1602
1603 # Function to estimate the spatial indicators:
1604 fun.indicators <- function(dat) {
1605   ## function to be used in this chunk:
1606   require(RGeostats);require(ineq) # For Gini index
1607   dat <- data.frame(dat)
1608   names(dat) <- c("x","y","pred")
1609
1610   if(max(dat$pred, na.rm=TRUE)!=0){
1611     dat$pred[dat$pred<0] = 0 #to avoid issues with center of gravity
1612     kk <- db.create(x1=dat$x, x2=dat$y, z1=dat$pred)
1613     kk2 <- SI.cgi(kk) # for the centre of gravity, inertia and isotropy-
1614     kk5 <- ineq(dat$pred, type="Gini")# gini index
1615     return(data.frame(t(unlist(kk2)[c(1,3,4,5)]), Gini=kk5))
1616   }}
1617
1618 # To test the function
1619 # fun.indicators(dat = rasterToPoints(pred[[1]]))
1620
1621
1622 # Function to apply the indicators function, estimate the difference between sampled and
1623 interpolated and estimate the data limits integrity measures:
1624 fun.inter2 = function(ii, dat=dat, pred=pred){
1625
1626   predi = rasterToPoints(pred[[ii]])
1627
1628   # Estimate the indicators of interpolated
1629   res2 <- fun.indicators(predi)

```

```

1630
1631 # Estimate the indicators for raw data
1632 res1 <- fun.indicators(dat[, c("x","y","vari")]) # 0.35 sec
1633
1634 # Absolute difference between sampled and interpolated
1635 res <- abs(res1-res2)
1636 names(res)[c(1,2,5)] = paste0("a.",names(res)[c(1,2,5)])
1637 res$method <- ii
1638
1639 # Diff of center of gravity
1640 res$CGdist <- spDistsN1(as.matrix(res1[,c("center1","center2")]),
1641 as.matrix(res2[,c("center1","center2")]))
1642
1643 # Rescale inertia
1644 res$a.linertia = log1p(res$a.inertia)
1645
1646 # Get number of pixels values over max biom pred
1647 ll <- dim(predi)[1] # number of pixels
1648 mx <- max(dat$vari, na.rm=TRUE)
1649 mm <- mean(dat$vari, na.rm=TRUE)
1650
1651 res$a.pix_under <-
1652   abs(ifelse(is.null(dim(predi[predi[,3]<0,])[1]),0,
1653     round(dim(predi[predi[,3]<0,])[1]/ll*100,2)))
1654
1655 res$a.pix_over <-
1656   abs(ifelse(is.null(dim(predi[predi[,3]> mx,])[1]),0,
1657     round((dim(predi[predi[,3] > mx,])[1]/ll)*100,2)))
1658
1659 res$a.mean_perc <- abs(round(c(mean(predi[,3], na.rm=TRUE)- mm)/mm * 100, 2))
1660
1661 res$a.over_perc <- abs(round((max(predi[,3], na.rm=TRUE)-mx)/mx*100,2))
1662
1663 res <- res[,c("method", "CGdist","a.linertia","a.iso","a.Gini",
1664   "a.pix_under","a.pix_over","a.mean_perc","a.over_perc")]
1665 return(res)
1666 }
1667
1668 # Function to make the PCA and estimate the best method according to the indicators
1669 PCbiplot <- function(datpc=sec.res,
1670   x="PC1", y="PC2") {
1671   require(ggrepel)
1672
1673   # exclude indicators with zero only
1674   datpc = datpc[,colSums(datpc)!=0]
1675
1676   # PCA
1677   PC <- prcomp(datpc, scale=TRUE, center=FALSE)
1678   #biplot(PC)
1679   data <- data.frame(winner2=row.names(PC$x),PC$x)

```

```

1680  datapc <- data.frame(varnames=rownames(PC$rotation), PC$rotation)
1681
1682  mult <- min((max(data[,"PC2"]) - min(data[,"PC2"])/(max(datapc[,"PC2"])-
1683 min(datapc[,"PC2"]))), (max(data[,"PC1"]) - min(data[,"PC1"])/(max(datapc[,"PC1"])-
1684 min(datapc[,"PC1"]))))
1685  datapc <- transform(datapc, v1 = .7 * mult * (get("PC1")), v2 = .7 * mult * (get("PC2")))
1686  dev <- paste0(c(round(((PC$sdev)^2 / sum(PC$sdev^2) ) * 100))[1:2], "%")
1687
1688  # Get distance to center of each point:
1689  data$dist <- apply(data[,c("PC1", "PC2")], 1,
1690                    function(x) {
1691                      (sqrt((x[1] - 0)^2 + (x[2] - 0)^2))
1692                    })
1693  # Reverse weights, as the closer to zero the better:
1694  data$dist2 <- 1/data$dist
1695
1696  # Classification and col of criteria
1697  col.ind <- data.frame(nam=row.names(datapc), class=1)
1698  col.ind[col.ind$nam %in% c("IMAE", "IRMSE", "VEcv.inv"), 2] <- "Error";
1699  col.ind[col.ind$nam %in% c("CGdist", "a.linertia", "a.iso", "a.Gini"), 2] <- "Spatial";
1700  col.ind[col.ind$nam %in% c("a.pix_under", "a.mean_perc", "a.over_perc", "a.pix_over"), 2] <-
1701  "Integrity"
1702  col.ind$nam = factor(col.ind$nam)
1703  col.ind$col = c("#5E4FA2", "#3288BD", "#66C2A5")[factor(col.ind$class)]
1704  #rev(brewer.pal(11, "Spectral"))
1705
1706  plot1 <-
1707  ggplot(data, aes(x=PC1, y=PC2)) +
1708  geom_point(aes(col=dist2), size = 1, shape=16)+
1709  geom_text_repel(aes(label = winner2, size=dist2, color=dist2)) +
1710  scale_colour_gradient(high = "#9E0142", low = "#FDAE61")+
1711  geom_hline(aes(yintercept=0), size=.2, color=8, linetype=2) +
1712  geom_vline(aes(xintercept=0), size=.2, color=8, linetype=2)+
1713  xlim(extendrange(c(data$PC1, datapc$PC1))[1], 0.01)+
1714  ylim(extendrange(c(data$PC2, datapc$PC2)))+
1715  # plot criteria:
1716  geom_text_repel(data=datapc, aes(x=v1, y=v2, label=varnames), size = 3,
1717  segment.alpha=.5,
1718  color=col.ind$col)+
1719  geom_segment(data=datapc, aes(x=0, y=0, xend=v1, yend=v2),
1720  arrow=arrow(length=unit(0.2, "cm")), color=col.ind$col)+
1721  xlab(paste0("PC1 (", dev[1], ")")+
1722  ylab(paste0("PC2 (", dev[2], ")")+
1723  ggtitle("PCA of indicators")+
1724  theme(line = element_blank(),
1725  axis.text=element_blank(),
1726  axis.ticks=element_blank()+
1727  scale_size(range = c(3, 5))+
1728  guides(size=FALSE, fill=FALSE, col=FALSE)
1729  plot2 <-

```

```

1730 ggplot(data, aes(x=reorder(winner2,dist2), y=dist2)) +
1731 geom_bar(stat="identity", aes(fill=dist2),col="White", alpha=.8)+
1732 scale_fill_gradient(high = "#9E0142", low = "#FDAE61")+
1733 theme(line = element_blank(),
1734        axis.text.y=element_blank(),
1735        axis.ticks.y=element_blank(),
1736        axis.text.x=
1737          element_text(angle=90,hjust=1))+
1738 xlab("Interpolation methods")+
1739 ylab("Inv. dist. to center")+
1740 ggtitle(" ") +
1741 guides(size=FALSE, fill=FALSE, col=FALSE)
1742
1743 grid.draw(arrangeGrob(plot1, plot2, ncol=2, widths = c(3/4,1/4)))
1744
1745 # Result's table
1746 kk <- data %>%
1747   dplyr::rename("method" = "winner2") %>%
1748   dplyr::mutate(dist2 = round(dist2,2)) %>%
1749   dplyr::select(method, dist2) %>%
1750   dplyr::arrange(dist2)
1751 return(kk)
1752 }
1753
1754
1755

```